

1 **Microbiome dysbiosis regulates the level of energy production under anaerobic condition**

2 M. Shaminur Rahman^{1#}, M. Nazmul Hoque^{1,2,#}, Joynob Akter Puspo¹, M. Rafiul Islam¹, Niloy
3 Das^{1,3}, M. Anwar Siddique¹, M. Anwar Hossain^{1,4}, Munawar Sultana^{1,*}

4

5 ¹Department of Microbiology, University of Dhaka, Dhaka-1000, Bangladesh

6 ²Department of Gynecology, Obstetrics and Reproductive Health, Bangabandhu Sheikh Mujibur

7 Rahman Agricultural University, Gazipur-1706, Bangladesh

8 ³Surge Engineering (www.surgeengineering.com), Dhaka-1205, Bangladesh

9 ⁴Present address: Jashore University of Science and Technology, Jashore-7408, Bangladesh

10

11 #Equal Contribution

12 *Correspondence to: Munawar Sultana, Associate Professor, Department of Microbiology,

13 University of Dhaka, Bangladesh. E-mail:munawar@du.ac.bd

14

15

16

17

18

19

20

21

22

23

24

25 **Abstract**

26 The microbiome of the anaerobic digester (AD) regulates the level of energy production.
27 To assess the microbiome dysbiosis in different stages of anaerobic digestion, we analyzed 16
28 samples dividing into four groups (Group-I = 2; Group-II = 5; Group-III = 5 and Group-IV = 4)
29 through whole metagenome sequencing (WMS). The physicochemical analysis revealed that
30 highest CH₄ production (74.1%, on Day 35 of digestion) was associated with decreased amount of
31 non-metal (phosphorus and sulfur) and heavy metals (chromium, lead and nickel). The WMS
32 generated 380.04 million reads mapped to ~ 2800 distinct bacterial, archaeal and viral genomes
33 through PathoScope (PS) and MG-RAST (MR) analyses. The PS analysis detected 768, 1421,
34 1819 and 1774 bacterial strains in Group-I, Group-II, Group-III and Group-IV, respectively which
35 were represented by *Firmicutes*, *Bacteroidetes*, *Proteobacteria*, *Actinobacteria*, *Spirochaetes* and
36 *Fibrobacteres* (> 93.0% of the total abundances). The archaeal fraction of the AD microbiomes
37 was represented by 343 strains, of which 95.90% strains shared across these metagenomes. The
38 indicator species analysis showed that *Methanosarcina vacuolate*, *Dehalococcoides mccartyi*,
39 *Methanosarcina* sp. Kolksee and *Methanosarcina barkeri* were the highly specific for energy
40 production in Group-III and Group-IV. However, most of the indicator phylotypes displayed
41 reduced abundance in the initial stage of biogas production (Group-I and Group-II) compared to
42 their increased relative abundances in Group-IV (Day 35). The correlation network analysis
43 showed that different strains of *Euryarcheota* and *Firmicutes* phyla were associated with highest
44 level (74.1%) of energy production (Group-IV). In addition to taxonomic dysbiosis, top CH₄
45 producing microbiomes showed increased genomic functional activities related to one carbon and
46 biotin metabolism, oxidative stress, proteolytic pathways, MT1-MMP pericellular network, acetyl-
47 CoA production, motility and chemotaxis. This study reveals distinct changes in composition and

48 diversity of the AD microbiomes including different indicator species, and their genomic features
49 that are highly specific for energy production.

50

51 **Introduction**

52 Bangladesh is experiencing rapidly increased energy consumption over the past two
53 decades. Being one of the world's most densely populated and least urbanized countries, around
54 72% of population of this country live in rural areas where there is no supply of natural gas, the
55 main source of energy [1]. The access to clean and affordable energy is one of the prerequisites to
56 achieve the sustainable development in rural areas. Upgrading existing biomass resources (i.e.,
57 animal manure, crop residues, kitchen and green wastes) to biogas shows significant promise in
58 this respect [2]. The production of biogas through anaerobic digestion process cannot only provide
59 fuel, but is also important for reduction of fertilizer nutrient utilization, rural forest conservation,
60 protecting the environment, realizing agricultural recycling, as well as improving the sanitary
61 conditions, in rural areas [3,4]. Biogas, produced from anaerobic digester (AD) is a relatively
62 high-value fuel and continuous source of energy supply, and insurance of future energy in a
63 sustainable manner [5]. Anaerobic environments play critical roles in the global carbon cycle
64 through the digestion of organic agricultural waste, manure, municipal waste, digester materials,
65 sewage, green waste or food. Biogas can significantly contribute to abate greenhouse gas emissions
66 from livestock and agricultural farming at relatively lower mitigation costs. However, attention
67 must be paid towards undesired emissions of methane (CH_4) and nitrous oxide (N_2O) from manure
68 storage [6]. Moreover, anaerobic digestion of livestock manure improves organic fertilizer quality
69 compared with undigested manure [7], and the load of the pathogenic microorganisms and related
70 antimicrobial resistance is also decreased through the biological process of anaerobic degradation

71 [8]. The rising energy prices and increasing concern of emission of greenhouse gases are the major
72 concern for the people and agro-industries worldwide to consider the wider application of AD
73 technology. This sustainable technology has been viewed as a way to address environmental
74 concern through the generation of CH₄ within engineered bioreactors, and thereby reducing the
75 human dependence on fossil fuels [9,10]. The conversion of organic wastes, agricultural residues
76 and renewable primary products into energy and other valuable products AD by the efficient
77 process of the AD is also considered as a sustainable solution for resource recovery and renewable
78 energy production underpinning the circular economy concept [9]. Furthermore, environment
79 friendly renewable energy produced from locally available raw materials and recycled waste could
80 thus contribute to climate change mitigation [5].

81 The renewable energy (CH₄) produced from the anaerobic bioreactor (AD) which is
82 independent of weather conditions could serve for the production of electricity, heat and fuels [11].
83 Anaerobic transformation of organic wastes in the AD is carried out by different bacterial and
84 archaeal species, such as hydrolytic, acid forming, acetogenic, and methanogens which produce
85 CO₂ and CH₄ as the main products of the digestion process [9]. Methane rich biogas (typically 50
86 – 70% methane, 30–50% CO₂, with traces of H₂S and other gases) is a clean, efficient, and
87 renewable source of energy, which offers a multipurpose carrier of energy, and can be used as a
88 substitute for other fuels [12]. Though biogas (CH₄) is directly influenced by the composition of
89 the AD microbiomes [9,13], the genomic potentials of the microbiomes favoring anaerobic
90 metabolism to control the level of CH₄ production is thermodynamically dependent on
91 environmental parameters of the AD [14]. Diverse microbial communities are associated with
92 biomass decomposition and CH₄ production through the metabolic activities of substrate
93 hydrolysis, acidogenesis, acetogenesis and methanogenesis [15]. The environmental and internal

94 factors such as substrate ingredients, temperature, pH, level of CO₂, O₂ and H₂S, and mixing or
95 the geometry of the AD can be achieved through microbial selection or manipulation [9,13,16].
96 Therefore, a clear understanding of the structure, composition and diversity of the multifarious
97 microbial community involved in biogas production is crucial for the optimization of their
98 performance and stable operational process of the AD. Moreover, a detailed insight into relevant
99 microbial metabolic pathways involved in CH₄ synthesis and syntrophy is essential to upsurge the
100 yield of biogas. To reveal the dynamic changes of the exceedingly diverse and unified networks
101 of AD microbiomes, few studies focused on the taxonomic and functional characterization of
102 microbiomes originating from both laboratory-scale [9] and full-scale [9,17] biogas reactors under
103 different prevailing ecological conditions [13,18]. Initially, AD microbiomes characterization
104 mainly relied on conventional microbiology approaches. However, at the very beginning of the
105 twentieth century more than 150 species of microorganisms have been identified from the
106 anaerobic bioreactors through the application modern genomic approaches [19]. The current
107 accelerated pace of genomic technology and the rapid incorporation of biotechnological techniques
108 allowed us the rapid identification and characterization microorganisms such as *Clostridium*
109 *bornimense*, *Herbinix hemicellulosilytica*, *Herbinix luporum*, *Herbivorax saccincola*,
110 *Proteiniphilum saccharofermentans*, *Petrimonas mucosa*, *Fermentimonas caenicola*, and
111 *Proteiniborus indolifex* or even their genomic features for the increased production of biogas
112 [9,13,17,19-21]. The conventional culture-based techniques [22,23] for characterization of the
113 microbiotas in different niches including controlled anaerobic chambers [11,24] has been replaced
114 during the last decade by the rapid advances in high-throughput NGS technology and
115 bioinformatics tools [25,26]. Despite, the 16S rRNA partial gene sequencing approach remained
116 the most widely used genomic approach to study the microbiomes of the AD [12,27], several

117 inherent limitations including the polymerase chain reaction (PCR) bias, inability to detect viruses,
118 lower taxonomic resolution (up to genus level only), and limiting information on gene abundance
119 and functional profiling have made this technique questionable [25,26]. Conversely, the whole
120 metagenome sequencing (WMS) or shotgun approach which can identify the total microbial
121 components of a sample (including viruses, bacteria, archaea, fungi, and protists) is being used
122 prudently to decipher the phylogenetic composition, microbiome structure and diversity including
123 profiling of their functional characteristics and interconnections [12,28].

124 To address the dynamic shifts in microbiome diversity and composition to be associated
125 with different level of renewable energy production in the controlled AD, we present a
126 comprehensive deep metagenomic (WMS) analysis of sixteen (n=16) samples collected from the
127 same AD under different pH, CO₂, O₂ and H₂S levels and temperature. Using a homogeneous
128 mapping and annotation workflow associated with a de-replication strategy, our analyses identified
129 ~ 2800 distinct bacterial and archaeal species along with their co-presence networking,
130 antimicrobial resistance and metabolic functional profiling. This study therefore provides an
131 opportunity to in-depth study the genetic potential and performance of microbial taxa represented
132 by WMS, and to relate their activities to generate renewable energy under changing environmental
133 conditions and process parameters.

134 **Materials and methods**

135 **Digester setup and experiment design**

136 The experiment was conducted using an anaerobic digester (AD) plant prepared with
137 provisions to measure temperature, slurry and gas sample collection and substrate charging. The
138 biogas plant consisted of a digester, inlet-chamber, three slurry outlet pipes, gas outlet pipe and
139 thermometer (Fig S1). The AD that contains the substrate (organic wastes) and converts it into

140 biogas and slurry was of 3000 L capacity, and made of flexible polyvinyl chloride (PVC) fabric
141 with thickness: 1.2mm. There was a specialized ball valve which ensures the anaerobic condition
142 within the digester and control the flow of substrates. The temperature of the AD was monitored
143 using a probe. The experiment was conducted for 45 days (Day 0 to Day 44, July 15 to August 27,
144 2019). The AD was charged 14 times during first 36 days (Day 0-35) with 1,192 kg raw cow dung
145 (highest input volume = 375 kg and lowest input volume = 35 kg) (Table S1). Initially, the digester
146 was started with charge of 375 kg feedstock where the ratio of raw cow dung and active sludge
147 was 1:1. The raw semi-solid cow dung (CD) was mixed with seed sludge from previous biogas
148 plant (slurry) before charged into the AD. The AD was portable, light in weight, low cost and
149 retains more heat inside.

150 **Sample collection and physicochemical parameters analysis**

151 The representative samples (n=16) including CD, slurry and active sludge (AS) were
152 collected and stored for subsequent analysis. The samples were categorized into four groups
153 (Group-I, Group-II, Group-III and Group-IV) based on collection time (Day 0 to Day 35) and CH₄
154 concentration. The samples of Group-I (n = 2) were collected at Day 0 (day of first input) when
155 the CH₄ concentration of the digesta was 0.0% with an average pH of 5.44. Likewise, Group-II
156 samples (n = 5) were collected at Day 2 and Day 7 of the digestion process when the CH₄
157 concentration and pH of the digesta were 21% and 5.44, and 34% and 5.56, respectively. The
158 sampling of the Group-III (n = 5) was done at Day 10 and Day 27 of the digestion process having
159 the CH₄ concentration and pH of the digesta 47.4% and 5.97, and 58.2% and 6.87, respectively.
160 The Group-IV included samples (n = 4) collected at Day 34 and Day 35 of digestion when the CH₄
161 concentration and pH of the digesta were 71.4% and 6.99, and 74.1% and 7.01, respectively (Table
162 1). Therefore, highest CH₄ production (74.1%) was recorded at Day 35 of the digestion process.

163 In addition, data on physicochemical parameters were recorded up to Day 45 (Table 1). Total
 164 nitrogen (TN) content was measured by micro-Kjeldahl method [29] while phosphorus, potassium,
 165 heavy metals (Lead, Zinc, Nickel, Cadmium, Chromium), organic carbon, Sulphur and moisture
 166 content were determined by spectrophotometric molybdovanadate [30], flame photometric [31],
 167 atomic absorption spectrophotometric [30], wet oxidation, turbidimetric and gravimetric methods
 168 from the Department of Soil Science, University of Dhaka. The detection limit of metals was of
 169 the order of 0.1 $\mu\text{g L}^{-1}$ [32].

170 **Table 1:** Metagenome samples and their groupings in the anaerobic digester according to
 171 experiment time and methane (CH₄) concentration.

Sample ID	Groups	Day	CH ₄ (%)	pH	Purity (280/260)	Concentration (ng/ μL)
R1	Group-I	0	0	5.43	1.78	103.7
M3				5.46	1.82	91.7
O4	Group-II	2	21	5.44	1.88	61
I5					1.88	77.7
M6					1.87	73.4
O7		7	34	5.56	1.87	46
I9					1.88	87.2
O10					1.87	48.6
M11	Group-III	10	47.4	5.97	1.86	86.1
I12					1.88	100.5
O60					27	58.2
O13		1.89	61.3			
O15		Group-IV	34	71.4	6.99	1.81
I14	1.82					65.4
O16	35		74.1	7.01	1.81	112.3
I17					1.81	53.6

172 *R1 = Raw cow dung, M3 = mixtures with raw cow dung and slurry from previous biogas plant
 173 as seed, O = Outlet samples, I = Input position samples, M = Middle position samples.

174 **Metagenomic DNA extraction, sequencing and bioinformatics analysis**

175 We extracted the total genomic DNA (DNA) from 16 samples (Data S1) using an
176 automated DNA extraction platform with DNeasy PowerSoil Kit (QIAGEN, Germany) according
177 to manufacturer's instructions. Extracted gDNA was quantified and purity checked through
178 NanoDrop (ThermoFisher, USA) with an absorbance ratio of 260/280. Shotgun metagenomic
179 (WMS) libraries were prepared with Nextera XT DNA Library Preparation Kit (Hoque et al.,
180 2019), and paired-end (2×150 bp) sequencing was performed on a NovaSeq 6000 sequencer
181 (Illumina Inc., USA) from the Macrogen Inc. (www.macrogen.com) Seoul, Republic of South
182 Korea. The gDNA from sixteen samples generated 380.04 million reads, and the average reads per
183 sample was 23.75 million (maximum = 24.79 million, minimum = 20.75 million) (Data S1). The
184 low-quality reads from the generated FASTQ files were filtered and removed through BBduk
185 (with options $k = 21$, $mink = 6$, $ktrim = r$, $ftm = 5$, $qtrim = rl$, $trimq = 20$, $minlen = 30$, $overwrite$
186 $= true$) (Stewart et al. 2018). In this study, on an average 21.45 million reads per sample
187 (maximum=23.75 million, minimum=18.85 million) passed the quality control step (Data S1).
188 Less than 100 hits were filtered for the downstream analysis. Read normalization in each sample
189 was performed using median sequencing depth through Phyloseq (version 4.0) package in R.

190 **Microbiome analysis and AMR profiling**

191 The taxonomic assignment of the generated WMS data was performed using both mapping
192 based and open-source assembly-based hybrid methods of PahtoScope 2,0 (PS) [33] and MG-
193 RAST 4.0 (MR) [34]. In PS analysis, the NCBI Reference Sequence Database (NCBI RefSeq
194 Release 201) for bacteria and archaea was prepared by Kraken2 [35]. The reads were then aligned
195 against the target (RefSeq) libraries using Minimap2 [36], and filtered to remove the reads aligned
196 with the cattle genome (bosTau8) and human genome (hg38) using BWA [37] and samtools [38].

197 In PS analysis, we employed the PathoID module to get exact read counts for downstream analysis
198 [33]. We simultaneously uploaded the raw sequences to the MR server with proper metadata. In
199 MR analysis, the uploaded raw reads were subjected to optional quality filtering with dereplication
200 and host DNA removal, and finally annotated for taxonomic assignment.

201 The within sample (alpha) diversity of microbial communities was calculated using the
202 Shannon and Simpson diversity indices [39] through the “Vegan” package in R. To evaluate alpha
203 diversity in different groups, we performed the non-parametric test Kruskal-Wallis rank-sum test.
204 The diversity across the sample groups (Beta-diversity) was measured with the principal
205 coordinate analysis (PCoA) using Bray–Curtis dissimilarity matrices, and permutational
206 multivariate analysis of variance (PERMANOVA) with 999 permutations to estimate a p-value for
207 differences among groups [40]. Phyloseq and Vegan packages were employed for these statistical
208 analyses [41]. Indicator species specific to a given sample group (having ≥ 1000 reads assigned to
209 a taxon) were identified based on the normalized abundances of species using the R package
210 indicpecies [42], and the significant indicator value (IV) index was calculated by the 999-
211 permutation test. Larger IV indicates greater specificity of taxa and $p < 0.05$ was considered
212 statistically significant [42]. Network analysis was used to explore the co-occurrence patterns of
213 the energy producing bacterial and archaeal taxa across the metagenome groups. In addition, the
214 Spearman’s correlation coefficient and significance tests were performed using the R package
215 Hmisc. A correlation network was constructed and visualized with Gephi (ver. 0.9.2).

216 We detected the antibiotics resistance genes (ARGs) among the microbiomes of four
217 metagenomes through the ResFinder 4.0 database (<https://doi.org/10.1093/jac/dkaa345>). The
218 ResFinder database was integrated within AMR++ pipeline [43] to identify the respective genes
219 and/or protein families [28]. In addition, the OmicCircos (version 3.9) [28], an R package was

220 used for circular visualization of both diversity and composition of ARGs across the metagenomes
221 under study.

222 **Functional profiling of the microbiomes**

223 In addition to taxonomic annotations, the WMS reads were also mapped onto the Kyoto
224 Encyclopedia of Genes and Genomes (KEGG) database [44], and SEED subsystem identifiers,
225 respectively, on the MR server [34] for metabolic functional profiling. The functional mapping
226 was performed with the partially modified set parameters (*e*-value cutoff: 1×10^{-30} , min. % identity
227 cutoff: 60%, and min. alignment length cutoff: 20) of the MR server [28].

228 **Statistical analysis**

229 To evaluate differences in the relative percent abundance of taxa in AD (Group-I, Group-
230 II, Group-III and Group-IV) for PS data, we used the non-parametric test Kruskal-Wallis rank sum
231 test. We normalized the gene counts by dividing the number of gene hits to individual taxa/function
232 by total number of gene hits in each metagenome dataset to remove bias due to differences in
233 sequencing efforts. The non-parametric test Kruskal-Wallis rank sum tests were also performed to
234 identify the differentially abundant SEED or KEGG functions (at different levels), and
235 antimicrobial resistance (ARGs) in four metagenomes. All the statistical tests were carried out
236 using IBM SPSS (SPSS, Version 23.0, IBM Corp., NY USA). To calculate the significance of
237 variability patterns of the microbiomes (generated between sample categories), we performed
238 PERMANOVA (Wilcoxon rank sum test using vegan 2.5.1 package of R 3.4.2) on all four sample
239 types at the same time and compared them pairwise. A significance level of $\alpha = 0.05$ was used
240 for all tests.

241

242

243 **Results**

244 **Physicochemical properties of substrate and digesta**

245 The physicochemical properties of the digester feedstock before and after the anaerobic
246 digestion of cow dung are shown in Figure 1 and Table 2. The fermentation was run for 44 days.
247 Periodic increments of the organic loading rate (OLR) resulted in increased biogas production (Fig
248 1A, Table S1). This trend was observed until Day 35, after which biogas production began to
249 decline gradually, although the OLR was kept constant. The lag phase of methane (CH₄)
250 production started around the second day of the experiment, and reached its maximum percentage
251 (74.1%) at Day 35 of the digestion process. It should be pointed out that after Day 35, the CH₄
252 percentage started to decrease, reaching 59.2% on Day 44 (Table 1). Average concentration (%)
253 CO₂ was observed 39.52 (minimum = 27.7, maximum = 56) throughout 44 days of the digestion
254 process. Concentration of H₂S was maximum (938 ppm) at Day 3, and later on the concentration
255 fluctuated based on feeding (Fig 1A, Table S1). The overall environmental temperature, AD
256 temperature, AD pressure and humidity were 34.75 °C (maximum = 38.8 °C, minimum = 32.0
257 °C), 34.46 °C (maximum = 51.0 °C, minimum = 0.0 °C), 22.52 mb (maximum = 56.41 mb,
258 minimum = 0.0 mb), and 55.5 % (maximum = 94.0 %, minimum = 42.0 %) (Fig 1B, Table S2).
259 On Day 35 of the digestion, when maximum methanogenesis was observed, the concentration of
260 organic carbon (OC) and total nitrogen (TN) in the fermentation pulp were 15.48% and 1.22%,
261 respectively, whereas the concentration of OC and TN in the slurry (CD + seed sludge; Day-0)
262 were 34.39% and 1.96%, respectively (Table 2). The overall C/N ratio of the feedstock also
263 gradually decreased with the advent of anaerobic digestion process, and found lowest (12.7:1) at
264 Day 35. Similarly, the amount of non-metallic element (phosphorus and sulfur) and heavy metals
265 (chromium, lead and nickel) content significantly decreased at the Day 35 of the digestion process

266 (Table 2). However, the amount of zinc and copper did not vary significantly throughout the
267 digestion period (Table 2).

268 **Table 2:** Physicochemical properties of raw cow dung, slurry and active sludges.

Parameters	Cow dung (CD; Day-0)	Slurry (CD + seed sludge; Day-0)	Active sludge (AS; Day-35, highest CH ₄ concentration)
Moisture (%)	23.32	86.16	90.03
Organic carbon (%)	34.39	36.83	15.48
Total nitrogen (%)	1.82	1.96	1.22
C: N	18.9:1	18.8:1	12.7:1
Phosphorus (%)	0.249	0.461	0.070
Sulphur (%)	0.522	0.579	0.038
Zinc (mg/kg)	16.24	17.56	15.58
Copper (mg/kg)	2.88	3.59	2.13
Chromium (mg/kg)	11.97	11.33	0.23
Cadmium (mg/kg)	BDL	BDL	0.04
Lead (mg/kg)	3.44	3.26	1.06
Nickel (mg/kg)	3.28	6.70	0.34

269 CD: raw semi-solid cow dung which was mixed with water; Slurry: mixture of CD and seed sludge
270 from previous biogas plant; AS: slurry from the AD when the gas production rate was the highest (i.e.
271 74.1% CH₄ concentration); and BDL: below detection limit.

272

273 **Microbiome composition and diversity in anaerobic digester**

274 The whole metagenome sequencing (WMS) of 16 sample libraries resulted in 380.04
275 million reads passing 343.26 million reads quality filters, which corresponded to 90.32% total
276 reads (individual reads per sample are shown in Data S1). The major microbial domain in all
277 samples was Bacteria with an abundance of 81.80%, followed by archaea (15.43%), and viruses
278 (2.77%) (Data S1).

279 The alpha diversity (i.e., within-sample diversity) of the AD microbiomes was computed
280 using the Shannon and Simpson estimated indices (i.e., a diversity index accounting both evenness

281 and richness) at the strain level. In this study, both Shannon and Simpson indices estimated
282 diversity significantly varied across the four sample groups ($p = 0.03541$, Kruskal-Wallis test).
283 The pair-wise comparison of the within sample diversity revealed that the microbiomes of the
284 Group-II significantly differed with those of Group-III and Group-IV ($p= 0.048$, Wilcoxon rank
285 sum test for each) compared to Group-I ($p= 0.91$, Wilcoxon rank sum test) (Fig 2A, B). The
286 rarefaction analysis of the observed species showed a plateau after, on average, 21.45 million reads
287 (Fig S2, Data S1)-indicating that the coverage depth for most samples was sufficient to capture the
288 entire microbial diversity. We also observed significant differences in the microbial community
289 structure among the four metagenome groups (i.e., beta diversity analysis). Principal coordinate
290 analysis (PCoA) at the strain level (Fig 2C), showed a distinct separation of samples by the
291 experimental groups. Besides, we found significant ($p = 0.032$, Kruskal Wallis test) differences in
292 the abundance of ARGs and metabolic functional genes/pathways (Data S2) which could strongly
293 modulate the level of energy production through microbiome dysbiosis in the AD.

294 In this study, on an average 0.43% WMS reads (assigned for r RNA genes) mapped to 28,
295 110 and 552 bacterial phyla, orders and genera respectively, and relative abundance of the
296 microbiome differed significantly ($p = 0.034$, Kruskal-Wallis test) across the metagenome groups
297 (Data S1). We observed significant shifts/dysbiosis in the microbiome composition at strain level.
298 The PS analysis detected 2,513 bacterial strains across the four metagenomes, of which 768, 1421,
299 1819 and 1774 strains were found in Group-I, Group-II, Group-III and Group-IV metagenomes,
300 respectively. Only, 18.34% detected strains were found to be shared across the four energy
301 producing metagenomes (Fig 3, Data S1). The archaeal fraction of the AD microbiomes was
302 represented by 5, 17, 61 and 343 archaeal phyla, orders, genera and strains, respectively, and the
303 relative abundance of these microbial taxa also varied significantly among the four metagenome

304 groups. Remarkably, 95.90% (329/343) of the detected archaeal strains shared across these
305 metagenomes (Fig 3, Data S1). In addition, 472, 536, 535 and 536 strains of bacterial viruses
306 (bacteriophages) were identified in Group-I, Group-II, Group-III and Group-IV metagenomes,
307 respectively.

308 **Microbial community dynamically changed over time in the anaerobic digester**

309 Significant changes in the abundances of core microbial groups were observed under
310 anaerobic condition of the AD. At phylum level, the AD metagenome was dominated by
311 *Firmicutes*, *Bacteroidetes*, *Proteobacteria*, *Actinobacteria*, *Spirochaetes* and *Fibrobacteres*
312 comprising > 93.0% of the total bacterial abundances. Among these phyla, *Firmicutes* was the
313 most abundant phylum with a relative abundance of 41.94%, 37.99%, 40.40% and 38.96% in
314 Group-1, Group-II, Group-III and Group-IV, respectively. The relative abundance of
315 *Bacteroidetes* (from 37.87% in Group-I to 22.40% in Group-IV) and *Actinobacteria* (from 3.94%
316 in Group-I to 3.30% in Group-IV) gradually decreased with the advance of AD digestion time.
317 Conversely, relative abundance of *Proteobacteria* (from 8.08% in Group-I to 18.92% in Group-
318 IV) and *Spirochaetes* (from 1.28% in Group-I to 3.70% in Group-IV) gradually increased with the
319 increase of anaerobic digestion time in AD. The rest of phyla also differed significantly across
320 these four groups keeping comparatively higher relative abundances during highest CH₄ producing
321 stage (Group-IV) of the AD. Similarly, *Clostridiales* and *Bacteroidales* were identified as the top
322 abundant order in Group-1, Group-II, Group-III and Group-IV with a relative abundance of
323 32.37%, 27.81%, 29.22% and 27.87%, and 32.49%, 27.42%, 27.53% and 14.94%, respectively
324 (Data S1).

325 The structure and relative abundances of the bacteria at the genus level also showed
326 significant differences ($p = 0.031$, Kruskal-Wallis test) across the study groups. In Group-I, Group-

327 II and Group-III metagenomes, *Bacteroides* was the most abundant bacteria with a relative
328 abundance of 18.10%, 14.90% and 15.16%, respectively, but remained lower (8.31%) in Group-
329 IV samples. *Clostridium* was found as the second most predominant bacterial genus, and the
330 relative abundance of this bacterium was 11.92%, 11.13%, 11.73% and 12.15% in Group-1,
331 Group-II, Group-III and Group-IV, respectively. The relative abundance of *Ruminococcus*,
332 *Eubacterium*, *Parabacteroides*, *Fibrobacter*, *Paludibacter*, *Porphyromonas* and *Bifidobacterium*
333 gradually decreased with the increase of energy (CH₄) production rate, and remained lowest in
334 Group-IV. Conversely, *Candidatus*, *Bacillus*, *Treponema* and *Geobacter* showed an increasing
335 trend in their relative abundances gradually with the advance of digestion time and remained
336 lowest in relative abundances in Group-IV. The rest of the bacterial genera had lower relative
337 abundances in four metagenomes of the AD (Fig S3, Data S1).

338 In this study, *Methanosarcina* was the most abundant archaeal genus, and the relative
339 abundance of this genus remained two-fold higher in Group-III (35.84%) and Group-IV (36.53%)
340 compared to Group-I (17.52%) and Group-II (18.32%). Notably, the relative abundance of
341 *Methanoculleus* was found higher in Group-II (11.59%) and Group-IV (13.80%) and lowest in
342 Group-I (3.46%). Likewise, *Methanobrevibacter* was predominantly abundant at the initial phase
343 of digestion (highest in Group-I; 19.35%) and remained lowest in abundance in the top CH₄
344 producing metagenome (Group-IV; 5.01%). Besides these genera, *Methanothermobacter* (5.30%),
345 *Methanosaeta* (5.16%), *Methanococcus* (4.74%), *Thermococcus* (2.96%), *Methanocaldococcus*
346 (2.53%), *Pyrococcus* (2.35%), *Methanosphaera* (2.32%) *Methanococcoides* (2.10%) and
347 *Archaeoglobus* (2.01%) were the predominantly abundant archaeal genera in Group-I samples and
348 their relative abundances gradually decreased with the increase of energy production (Fig S4, Data
349 S1). On the other hand, *Methanoregula* (6.43%), *Methanosphaerula* (2.99%), *Methanoplanus*

350 (2.37%) and *Methanohalophilus* (1.39%) were the most abundant archaeal genera in Group-IV
351 metagenome. The rest of the genera remained much lower (< 1.0%) in relative abundances but
352 varied significantly across the four metagenomes (Fig S4, Data S1).

353 The strain-level composition, diversity and relative abundances of the microbiomes across
354 four metagenomes revealed significant variations ($p = 0.011$, Kruskal-Wallis test) (Fig 4, Data S1).
355 In this study, 2,513 bacterial and 343 archaeal strains were detected, of which 18.35% (461/2513)
356 bacterial and 95.92% archaeal strains shared across the study metagenomes (Fig 3, Data S1). Most
357 of the bacterial strains detected were represented by the phylum *Firmicutes* followed by
358 *Bacteroidetes*, *Gammaproteobacteria* and *Betaproteobacteria* (Fig S5, Data S1). Of the detected
359 strains, methanogenic archaeal strains were more prevalent (higher relative abundances) compared
360 to bacterial strains, and this strain-level microbiome profiling was more evident in highest energy
361 producing metagenome group (Group-IV). The most prevalent energy producing archaeal strains
362 in Group-IV were *Methanosarcina vacuolata* Z-761 (17.31%), *Methanosarcina* sp. Kolksee
363 (16.63%), *Methanoculleus marisnigri* JR1 (5.0%), *Methanothrix soehngenii* GP6 (4.61%),
364 *Methanobacterium formicicum* DSM 1535 (3.60%), *Methanoculleus* sp. MAB1 (2.07%) and
365 *Methanoculleus bourgensis* DSM 3045 (2.07%), and rest of strains had lower (< 2.0%) relative
366 abundances (Fig 4, Data S1). Moreover, the relative abundances of these strains gradually
367 increased with the increase of energy production (lowest relative abundance in Group-I and highest
368 relative abundance in Group-IV) (Data S1). Conversely, the relative abundances of most of the
369 bacterial strains identified gradually decreased with the advance of digestion time (increase of
370 energy production), and mostly remained higher in relative abundances in Group-I (Data S1). Of
371 the top abundant bacterial strains, *Bifidobacterium pseudolongum* subsp. *globosum* DSM 20092
372 (12.0%), *Phocaeicola dorei* DSM 17855 (6.61%), *Fibrobacter succinogenes* subsp. *succinogenes*

373 S85 (4.57%), *Faecalibacterium prausnitzii* M21/2 (2.89%), *Clostridiales bacterium* CCNA10
374 (2.78%), and *Flintibacter* sp. KGMB00164 (2.07%) were found in Group-I, and their abundances
375 gradually decreased with the increase of level of CH₄ production. In addition, *Dysosmobacter*
376 *welbionis* J115 (5.48%) remained more prevalent in Group-II (Fig 4, Data S1). The rest of the
377 bacterial strains were less abundant (<2.0%) across the four metagenomes (Fig 4, Data S1). The
378 viral fraction of the microbiomes mostly dominated by different strains of bacteriophages such as
379 *Gordonia* phage Secretariat (16.12%), *Streptomyces* phage Bing (5.33%) and *Arthrobacter* phage
380 Gordon (5.05%) in Group-I, *Megavirus chiliensis* (1.81%), *Acanthamoeba polyphaga*
381 moulmouvirus (1.60%) and *Orpheovirus* IHUMI-LCC2 (1.50%) in Group-II, *Stenotrophomonas*
382 phage Mendera (4.88%), *Choristoneura fumiferana* granulovirus (3.0%) and *Gordonia* phage
383 Secretariat (2.55%) in Group-III and *Stenotrophomonas* phage Mendera (2.58%), *Choristoneura*
384 *fumiferana* granulovirus (2.37%) and *Bacillus* phage Mater (1.47%) in Group-IV (Data S1).

385 **Identification of potential indicator species and their co-occurrence**

386 To identify microbial taxa (bacteria and archaea) that could discriminate across the four
387 metagenome groups of the AD in terms of energy production (% CH₄), the indicator species
388 analysis (ISA) was performed both in individual group and combination basis, as shown in (Fig
389 5). Indicator species were those which were significantly more abundant and present in all samples
390 belonging to one group, and also absent or low abundance in the other group (Fig 5, Data S1). The
391 core taxa were selected based on their relative frequency ($\geq 75\%$ occurrence in each of the four
392 groups) (Data S1). Although, 26, 3 and 19 indicator species were found in Group-I, Group-II and
393 Group-IV, respectively, and no indicator species were identified in Group-III (Fig 5A, Data S1).
394 Higher indicator values (IVs) suggested better performances in the microbial signature of the
395 assigned taxa. *Desulfosporosinus youngiae*, *Treponema caldarium*, *Pseudoclostridium*

396 *thermosuccinogenes*, *Dehalobacterium formicoaceticum*, *Methanofollis liminatans*,
397 *Methanoregula boonei*, *Syntrophomonas wolfei*, *Hungateiclostridium clariflavum*, *Candidatus*
398 *Cloacimonas acidaminovorans* and *Methanocorpusculum labreanum* were highly specific for
399 energy production in Group-IV (highest CH₄ production rate; 74.1%), with IVs of 0.983, 0.978,
400 0.949, 0.907, 0.887, 0.885, 0.882, 0.851, 0.795 and 0.786, respectively (Fig 5A; Data S1).
401 Considering the combined group effects of the indicator species associated with energy production,
402 our analysis revealed that *Methanosarcina vacuolate*, *Dehalococcoides mccartyi*, *Methanosarcina*
403 sp. Kolksee and *Methanosarcina barkeri* in Group-III + Group-IV (top CH₄ producing groups)
404 having IVs of 0.88, 0.887, 0.879 and 0.879, respectively were highly specific for energy production
405 (Fig 5B, Data S1). All of the indicator phylotypes displayed reduced abundance in the initial stage
406 of biogas production (Group-I and Group-II, lower CH₄ production rate) compared to their
407 increased relative abundance up to Day 35 of the experiment (in Group-III and Group-IV) (Data
408 S1).

409 We then visualized networks within each metagenome group of the AD for both positive
410 and negative co-occurrence relationships (Fig 6, Data S1). The correlation networks analysis was
411 performed based on the significantly altered species (n=106) in different groups as revealed by
412 indispecies analysis. This network analysis explored significant association (p = 0.021, Kruskal-
413 Wallis test) in the co-occurrence patterns of the energy producing microbial taxa (species and/or
414 strains) based on their relative abundances in four metagenome groups. In the correlation network
415 of four metagenomes; Group-I to Group-IV), *Firmicutes* and *Bacteroidetes* exhibited strongest
416 relation. The resultant network consists of 106 nodes (17 in Group-I, 58 in Group-II, 5 in Group-
417 III and 26 in Group-IV) which were clearly separated into four modules/clusters (Fig 6). Taxa in
418 the same group may co-occur under the same AD conditions (temperature, O₂ and H₂S percentage,

419 pressure and humidity). Across different metagenome groups of AD, *Firmicutes*, *Bacteroidetes*,
420 *Actinobacteria* and *Proteobacteria* were the top abundant phyla in Group-I and Group-II with a
421 cutoff of 1.0 while *Bacteroidetes* and *Chlorhexi* in Group-III, and *Euryarcheota* and *Firmicutes* in
422 Group-IV were designated as the top abundant phyla with a cutoff of 1.0 (Fig 6). However, when
423 moving down to the species-level in microbiome co-occurrence in the AD, keystone taxa were
424 much more consistent between networks with different correlation cutoffs. These results reveal
425 that applying the same conditions in the AD for energy production, network elements must happen
426 under careful consideration of the parameters used to delineate co-occurrence relationships. The
427 positive correlations between Group-I and Group-II were observed among the microbiomes of the
428 AD while Group-III and Group-IV showed negative correlations in terms of energy production
429 with the microbial taxa of other two groups (Fig 6). These findings therefore suggest that different
430 strains of *Euryarcheota* and *Firmicutes* phyla were negatively correlated but associated with
431 highest level of energy production (highest % of CH₄; Group-IV).

432 **Genomic functional potentials of the anaerobic microbiomes**

433 In this study, there was a broad variation in the diversity and composition of the
434 antimicrobial resistance genes (ARGs) (Fig 7, Data S2). The results of the present study revealed
435 significant correlation ($p = 0.0411$, Kruskal-Wallis test) between the relative abundances of the
436 detected ARGs and the relative abundance of the associated bacteria found in four metagenomes
437 (Data S2). ResFinder identified 49 ARGs belonged to 19 antibiotic classes distributed in 2,513
438 bacterial strains (Data S2). The Group-III microbiomes harbored the highest number of ARGs
439 (42), followed by Group-II (38), Group-IV (29) and Group-I (22) microbes (Fig 7, Data S2). The
440 tetracyclines (doxycycline and tetracycline) resistant gene, *tetQ* had the highest relative abundance
441 (23.81%) in Group-I associated bacteria followed by Group-II (22.85%), Group-III (16.49%) and

442 Group-IV (6.73%)–microbes. Macrolides (erythromycin and streptogramin B) resistant genes such
443 as *mefA* (16.80%), *mefB* (15.32%) and *msrD* (11.10%) had higher relative abundances in highest
444 CH₄ producing metagenome compared to other metagenome groups. The broad-spectrum beta-
445 lactams resistant gene, *cfxA2-6* was found as the common ARG among the microbiomes of four
446 metagenomes, displaying the highest relative abundance (35.58%) in inoculum (Group-I)
447 microbiota followed by Group-II (23.09%), Group-III (8.02%) and Group-IV (0.14%)
448 microbiomes. The rest of the ARGs also varied in their expression levels across the four
449 metagenomes, being more prevalent in the Group-III microbiomes (Fig 7). In addition to these
450 ARGs, the highest CH₄ producing microbiomes were enriched with the higher relative abundance
451 of genes coding for cobalt-zinc-cadmium resistance (18.85%), resistance to chromium compounds
452 (12.17%), arsenic (6.29%), zinc (4.96%) and cadmium (3.26%) resistance compared to the
453 microbes of other three metagenomes (Fig S6, Data S2). By comparing the possible mechanisms
454 of the detected ARGs, we found that antibiotic efflux pumps associated resistance had the highest
455 level of expression in the anaerobic microbiomes of the AD followed by antibiotic inactivation,
456 enzymatic inactivation and modification, antibiotic target protection/alteration, and folate pathway
457 antagonist-attributed resistance mechanisms (Fig S6, Data S2).

458 Functional metabolic profiling of the gene families of the same KEGG pathway for AD
459 microbiomes revealed significant differences ($p = 0.012$, Kruskal-Wallis test) in their relative
460 abundances, and positive correlation with level of energy production. Of the detected KO modules,
461 genes coding for CHO metabolism and genetic information and processing were top abundant,
462 however did not vary significantly across the metagenome groups. Remarkably, the relative
463 abundance of genes coding for energy metabolism, xenobiotics biodegradation and metabolism,
464 butanoate metabolism, citrate synthase (*gltA*), succinyl-CoA synthetase subunits (*sucC/D*),

465 pyruvate carboxylase subunits(*pycA*) and nitrogen metabolism gradually increased with the
466 increasing rate of CH₄ production, and had several-fold over expression among the microbiomes
467 of Group-IV. Conversely, fumarate hydratase (*fumA/B*), malate dehydrogenase (*mdh*) and bacterial
468 secretion system associated genes were predominantly overexpressed in Group-I related
469 microbiomes which gradually decreased with advance of digestion process, and remained more
470 than two-fold lower expressed in the peak level of CH₄ production (lowest in Group-IV) (Fig 8A,
471 Data S2).

472 We also found 41 statistically different ($p = 0.033$, Kruskal-Wallis test) SEED functions in
473 the AD microbiomes. Overall, the top CH₄ producing microbiomes (Group-III and Group-IV) had
474 higher relative abundances of these SEED functions compared lower CH₄ producing microbiomes
475 (Group-I and Group-II), except for regulation of virulence (highest in Group-I microbes; 17.08%),
476 gluconeogenesis (highest in Group-I microbes; 16.27%) and transposable elements (highest in
477 Group-I microbes; 17.28%) (Fig 8B, Data S2). The Group-IV-microbiomes (highest CH₄
478 producing) were enriched in genes coding for tetrapyrroles (17.42%), one carbon (10.29%) and
479 biotin (4.55%) metabolism, oxidative (18.76%) and osmotic (9.94%) stress, proteolytic pathway
480 (7.74%), MT1-MMP pericellular network (6.45%), acetyl-CoA production (5.33%) and motility
481 and chemotaxis (3.13%) compared to the microbes of the other metagenomes. The Group-I
482 microbiomes however had a higher abundance of SEED functions involved in protection from
483 ROS (16.28%), heat shock (18.31%) and NAD and NADP (19.03%) (Fig 8B, Data S2).

484 **Discussion**

485 This study is the first ever approach to reveal the dynamic shifts in microbiome
486 composition and abundances in different levels of biogas production under the anaerobic digestion
487 system using the state-of-the-art WMS technology along with analysis of the physicochemical

488 parameters in Bangladesh. Anaerobic digestion of organic wastes is favored by the metabolic
489 activities of different types of microorganisms including bacteria and archaea [32]. The
490 physicochemical parameters assessment of the AD before and after digestion revealed that biogas
491 production was in increasing trend up to Day 35 with periodic loading of slurry (Day 1, 2, 3, 8, 10,
492 14, 16, 24 and 35) at 1:1 ratio of raw cow dung and active sludge (Table S1). After 30 days of
493 incubation, we found that cow wastes produced highest amount of biogas (on Day 35, CH₄;
494 74.1%), and thereafter decrease gradually reaching 59.2% on Day 44 of processing (Fig 1). Biogas
495 production chiefly depends on the content and chemical nature of biodegradable matter. The
496 biochemical parameter of cow waste (slurry) reflects the presence of high content of readily
497 biodegradable organic matter in the first phases (up to Day 35) of anaerobic digestion [32]. The
498 CO₂ concentration (%) found to be varied throughout the digestion process keeping an average
499 value of 39.52%. Our analysis revealed that OC and TN content was higher at the time of loading
500 of slurry in the AD compared to that of highest biogas production stage (at Day 35). The amount
501 of carbon available of the substrate determines the maximum amount of CH₄ and CO₂ that can be
502 formed by anaerobic digestion [7]. Conversely, C/N ratio remained lowest in this peak stage of
503 CH₄ production. Organic carbon is essential for bacterial growth, and determining of the C/N ratio
504 is essential for optimal biogas production [45]. Moreover, the total content of phosphorus, Sulphur
505 and heavy metals (chromium, lead and nickel) also remained lowest at this highest stage of biogas
506 production (Day 35). Of note, the highest CH₄ producing microbiomes were enriched with the
507 higher relative abundance of genes coding for heavy metals (cobalt-zinc-cadmium, chromium
508 compounds, arsenic, zinc, and cadmium) compared to the microbes of other three metagenomes.
509 The lowest chromium, lead and nickel concentration during highest CH₄ producing stage might be
510 associated with their higher abundances of heavy metal resistance genes (Fig S6, Data S2), and

511 small concentrations of these metals found in the process are essential for microbial maintenance
512 [46,47]. Certain specific metals such as Sulphur, cobalt and nickel serve as cofactors in the
513 enzymes involved in the formation of CH₄ during anaerobic processing [48]. However, the
514 minerals (e.g. zinc and copper) content of the AD did not vary throughout the digestion process
515 revealing their important roles in various metabolic pathways of anaerobic digestion [46].

516 The within (alpha) and between (beta) sample diversity of the AD microbiomes showed
517 that that microbial dysbiosis in the AD is closely linked to different levels of biogas production.
518 Compared to loading phase of AD (Group-I), increased microbial diversity and species richness
519 was observed in the later phases (Group-II, Group-III and Group-IV) of anaerobic digestion. Beta
520 diversity also revealed a substantial microbial disparity in different levels of biogas production,
521 and segregated the samples accordingly. Despite having higher taxonomic resolutions, the
522 microbiomes of the AD remained inconsistent and fluctuates more in Group-II, Group-III and
523 Group-IV than those of Group-I metagenome. The taxonomic annotations of the four groups of
524 AD showed that they were a reservoir of bacteria, followed by archaea and viruses, which
525 corroborated the findings of other studies [49,50]. Among the identified domains, bacteria
526 dominated in abundance, comprising 81.80% of the total microbial populations, followed by
527 archaea (15.43%), while viruses (2.77%) comprised the least abundant population. The observed
528 high bacterial abundances suggest their crucial metabolic roles in biomass conversion and other
529 reactions within the reactor systems [50]. The identified affiliates of archaea were mostly
530 consumers of smaller substrates that were generated by the bacterial taxa. The archaeal species are
531 able to use different methanogenic routes to convert the substrates into methane gas. Nevertheless,
532 the main roles of the identified less abundant bacteriophages were unclear, though the strains could
533 have been active in degrading other microbial cells in the AD systems [49,50].

534 In this study, *Firmicutes*, *Bacteroidetes*, *Proteobacteria*, *Actinobacteria*, *Spirochaetes* and
535 *Fibrobacteres* were the most abundant bacterial phyla, and their relative abundance also varied
536 according to the level of energy production in the corresponding sample groups. The observed
537 community composition at phylum level, with dominance of *Firmicutes*, *Bacteroidetes* and
538 *Proteobacteria*, is in line with previous findings for biogas reactors [47]. The first three phases
539 (hydrolysis/cellulolysis, acidogenesis/fermentation and acetogenesis) of the anaerobic digestion
540 are solely performed by fermentative Bacteria. In this study, the bacterial phyla *Firmicutes* (37.0%
541 - 42.0%) and *Bacteroidetes* (22.0% - 38.0%) appeared to dominate biogas communities in varying
542 abundances depending on the apparent process conditions. The initial phase of the AD digestion
543 process involves hydrolytic reactions that convert large macromolecules into smaller substrates
544 [49]. In addition, the nature and composition of the substrates, availability of nutrients and
545 ammonium/ammonia contents can affect both the composition and diversity of the methanogenic
546 archaea [49]. Only certain methanogenic archaea are able to synthesize CH₄ from the end products
547 of bacterial fermentation. The performance and efficiency of these processes depend to a large
548 extent on the presence of appropriate and adequate microorganisms along with the
549 physicochemical conditions of the digester and quality of the substrates (organic materials) etc.
550 The degree and rate of degradation (hydrolysis, fermentation, acetogenesis, and methanogenesis)
551 and the biogas yield depend not only on the chemical and physical characteristics of the substrates,
552 but also on the chosen process parameter such as temperature, humidity and retention time, that
553 shape the composition of different microbial groups and communities that active in the process
554 (Schnürer, 2016).

555 During the anaerobic process *Clostridiales* and *Bacteroidales* were identified as the top
556 abundant order in all of the four metagenome groups. The syntrophic bacterial genera and strains

557 of *Clostridiales* order are consumers of 30% of the generated electrons, which bypasses the rate
558 limiting steps of the volatile fatty acids accumulation and contributes to AD stabilities [49,51]. In
559 anaerobic environments, *Clostridiales* has been reported as the main cellulose degrader [52], and
560 play important role in the hydrolysis step [47]. These findings are in line with many of the previous
561 reports [49,53] who reported the potential roles of these bacterial taxa in the efficient and increased
562 production of biogas under anaerobic condition [54]. In addition, bacteria belonging to the order
563 *Bacteroidales* have been suggested to be involved in the degradation of lignocellulose materials,
564 such as straw and hay, the chief component of cattle feed [54,55]. The identified affiliates of
565 *Bacteroidales* belong to *Bacteroidetes*, and are majorly known to ferment carbohydrates and
566 proteins, concomitantly releasing H₂ [46]. Moreover, *Bacteroides*, the predominating genus in the
567 AD coming from *Bacteroidales* order were observed to co-exist with methanogenic archaea
568 possibly to increase energy extraction from indigestible plant materials [46], and we hypothesize
569 that they are the key drivers of the observed β -diversities since the relative abundance of this genus
570 gradually decreased with the digestion process.

571 The digestion process of the AD was carried out by the integrated cross-kingdom
572 interactions since both bacteria and archaea were simultaneously detected in this WMS-based
573 study corroborating with several earlier reports [25,26,28]. The strain-level taxonomic profiling
574 revealed that methanogenic archaeal strains were more prevalent than bacterial strains. The
575 archaeal domain of the AD microbiomes was composed of different strains of methanogenic,
576 hydrogenotrophic and thermophilic genera of *Methanoculleus*, *Methanosarcina*, *Methanotherix*,
577 *Methanobacterium* and *Methanobrevibacter* genera. The current findings are corroborated with
578 many of the earlier studies who reported that these genera to be predominantly abundant in the AD
579 of manures [32], and associated with biogas production under anaerobic conditions [56]. These

580 methanogenic genera might reside in the microenvironments appropriate for anaerobic metabolism
581 [28] and their presence has been reported in microbial communities producing biogas [57].
582 Members of *Methanoculleus* are hydrogenotrophic methanogens [58], while *Methanosarcina*
583 species or strains are mostly acetoclastic but also able to use H₂ [12,59]. In addition,
584 *Methanosarcina* spp. has been reported to have higher growth rates and tolerance to pH changes
585 and could potentially lead to stable methanogenesis in the AD [8,60]. *Methanobrevibacter* was
586 predominant in initial phase of digestion (Day 2 and 15) in the bioreactor, and are known to be
587 hydrogenotrophic, by using CO₂ and H₂ as substrates to generate biomethane [12,57]. These
588 archaeal genera are suggested to play vital role in hydrogenotrophic methanogenesis, and
589 maintaining methanogenic community diversity [24,27].

590 Indicator species (IS) and network analyses were used to identify at higher taxonomic
591 resolution of the individual bacterial and/or archaeal species with enrichment or depletion patterns
592 in different phases of anaerobic digestion. These analyses revealed the association of different
593 methanogenic species with increased level of CH₄ production [61], and all were observed to be
594 more abundant in highest CH₄ producing metagenome (Group-IV). However, common indicator
595 bacteria *E. coli*, *Salmonella* and *Staphylococcus* species were not found in indicator species
596 analysis, and these findings are supported by several previous reports of the absence of common
597 indicator bacteria after 30 days digestion in the experimental AD at different temperatures (25 °C
598 - 45 °C) [62]. Spearman correlation analysis showed negative correlation between Group-II and
599 Group-IV microbiomes. These findings are in line with the metabolic functional potentials of the
600 AD microbiomes since fumarate hydratase (*fumA/B*), malate dehydrogenase (*mdh*) and bacterial
601 secretion system associated genes were predominantly overexpressed in Group-I and Group-III
602 microbiomes, which gradually decreased with advance of digestion process, and remained more

603 than two-fold lower expressed in highest CH₄ production stage (Group-IV) (Fig 8A, Data S2). The
604 microbial communities present in the early phase of digestion process (Group-I) increased both
605 composition and abundances in the second phase of digestion (Group-II metagenome) in ambient
606 growth conditions of the AD. With the advance of digestion time, the increasing efficiency of
607 anaerobic digestion creates a favorable environment for the methanogens (Figs 4 and 6), and thus
608 found in higher composition and abundances in Group-III and Group-IV metagenomes [24,27]. In
609 addition, the Group-IV-microbiomes showed higher genomic functional activities related to
610 tetrapyrroles, one carbon and biotin metabolism, oxidative and osmotic stress, proteolytic
611 pathways, MT1-MMP pericellular network, acetyl-CoA production, and motility and chemotaxis
612 compared to the microbes of the other groups. Though, these findings also support the taxonomic
613 dysbiosis of microbiomes in Group-IV metagenome, however further comprehensive study is
614 needed to elucidate the modulation of microbiome shifts, their functional potentials and genomic
615 expression using a larger dataset.

616 **Conclusions**

617 The level of biogas production increased gradually up to Day 35 (highest CH₄
618 concentration), and declined thereafter under controlled environment of the AD. With the increase
619 of CH₄ production, the amount of non-metallic elements (phosphorus and Sulphur) and heavy
620 metals (chromium, lead and nickel) decreases at Day 35 of the digestion process. The pair-wise
621 comparison of the within (alpha) and between (beta) sample diversities revealed that the
622 microbiomes of the Group-IV significantly differed with those of other three groups. The present
623 study revealed an imbalance distribution of bacterial phyla across four groups keeping
624 comparatively higher relative abundances and compositions of the methanogenic microbiomes
625 during highest CH₄ producing stage (Group-IV). The indicator species analysis revealed that

626 Group-III and Group-IV were highly specific for energy production. The correlation network
627 analysis of the indicator species showed that different strains of *Euryarcheota* and *Firmicutes*
628 phyla were negatively correlated but associated with highest level of energy production.

629

630

Figure Captions

631 **Fig 1:** Dynamic changes in the physicochemical parameters of the anaerobic digester (AD) over
632 the study period.

633

634 **Fig 2: Microbiome diversity in four metagenomic groups of the anaerobic digestate**
635 **samples.** Box plots showing significant differences in observed species richness in AD
636 associated microbiome. (A-B) Alpha diversity, as measured by PathoScope (PS) analysis using
637 the Shannon and Simpson diversity indices, revealed distinct microbiome diversity across four
638 metagenome samples ($p = 0.03541$, Kruskal-Wallis test). (C) The experimental groups were
639 clearly separated by principal coordinate analysis (PCoA), which was measured using non-
640 metric multidimensional scaling (NMDS) ordination plots. The different shapes represent the
641 assigned populations in four metagenomes. As the day progresses, the group color becomes
642 lighter. Values in parentheses represent the fraction of the total variance explained by each
643 PCoA axis.

644

645 **Fig 3: Unique and shared taxonomic composition of AD associated microbiome.** Four
646 metagenomics samples were represented by Venn diagrams depicting the core unique and
647 shared microbiomes. (A) Venn diagram showing unique and shared bacterial strain by PS
648 analysis, (B) Venn diagram showing unique and shared archaeal strain by PathoScope analysis.
649 Microbiome sharing between the conditions are indicated by red circles. More information on
650 the taxonomic result is also available in Data S1.

651 **Fig 4: The strain level taxonomic abundance of anaerobic digestion driving microbiome.**
652 Stacked bar plots showing the relative abundance and distribution of the 30 most abundant strains,
653 with ranks ordered from bottom to top by their increasing proportion among the four
654 metagenomics groups. Only the 29 most abundant strains are shown in the legend, with the
655 remaining strains grouped as 'Other strains'. Each stacked bar plot represents the abundance of
656 bacteria in each sample of the corresponding category. The relative abundances of archaeal strains
657 (red colored) steadily improved as energy demand increased (lowest relative abundance in Group-I
658 and highest relative abundance in Group-IV). In contrast, the relative abundances of most of the
659 known bacterial strains gradually decreased with the passage of time (increased energy
660 production), and mostly remained higher in Group-I and lower in Group-IV.

661

662

663 **Fig 5: Indicator species analysis of AD microbiome within four metagenomics groups.** (A)
664 Individual group effects of the indicator species associated with energy production, (B)
665 combined group effects of the indicator species associated with energy production. Indicator
666 values (IndVal) are shown next to the taxonomic information for the indicator taxa as indicated
667 by Indicator. Size of symbol is proportional to the mean relative abundance in that group of
668 AD. Red symbols indicate for which group the taxon is an indicator. Gray symbols indicate
669 group that contain a taxon, but for which that taxon is not an indicator taxa. Higher indicator
670 values (IVs) suggested better performances in the microbial signature of the assigned taxa.

671
672 **Fig 6: Microbiome co-occurrence in the AD within the four metagenomic groups.** The
673 microbiomes of the AD showed positive associations between Groups I and II, while Groups III
674 and IV showed negative correlations in terms of energy production with the microbial taxa of the
675 other two groups. Nodes are colored by taxonomy with labelled genera names. The positive
676 correlation is represented by the green line, while the negative correlation is represented by the red
677 line.

678 **Fig 7: Antibiotics resistance genes (ARGs) detected in anaerobic digestion driving**
679 **microbiome.** The circular plot illustrates the distribution of 49 ARGs belonged to 19 antibiotic
680 classes found across the four metagenomes. ARGs in the respective metagenome group are
681 represented by different colored ribbons, and the inner blue bars indicate their respective relative
682 abundances. Group-III associated microbiomes had the highest number of VFGs followed by
683 Group-II, Group-IV and Group-I microbes.

684
685 **Fig 8: Functional genomic potentials of the anaerobic digestion associated microbial**
686 **community through KEGG and SEED Pathways analysis.** (A) Heatmap depicting the
687 distribution of the 40 genes associated with the identified metabolic functional potentials detected
688 by KEGG Pathways analysis within the four metagenomic groups of the AD microbiome. (B)
689 Heatmap showing the distribution of the 41 functional gene composition and metabolic potential
690 detected by SEED Pathways analysis within the four metagenomic groups of the AD microbiome.
691 The color code indicates the presence and completeness of each gene, expressed as a value (Z
692 score) between -2 (low abundance), and 2 (high abundance). The red color indicates the highest
693 abundance whilst light green cells account for lower abundance of the respective genes in each
694 metagenome.

695
696
697

698

699 **Acknowledgements**

700 This project is financed by the Surge Engineering (www.surgeengineering.com)
701 Bangladesh.

702 **Supplementary Information**

703 Supplementary information supporting the results of the study are available in this article
704 as Data S1 and S2, Figs. S1-S6, and Table S1.

705 **Author Contributions**

706 MNH performed bioinformatics analysis, visualized figures, interpreted results and drafted
707 the original manuscript. MSR carryout field experiment, curated the data and performed
708 bioinformatics analysis. JAP carryout field experiment, and physicochemical analysis. MRI and
709 MAS edited the drafted manuscript. ND, MAH and MS conceived the study and critically
710 reviewed the drafted manuscript.

711 **Competing Interests**

712 The authors declare no competing interests.

713 **Data availability**

714 The sequence data reported in this article have also been deposited in the National Center
715 for Biotechnology Information (NCBI) under BioProject accession number PRJNA668799.

716 **Ethics Statement**

717 Not applicable

718

719

720

721

722

723

724 References

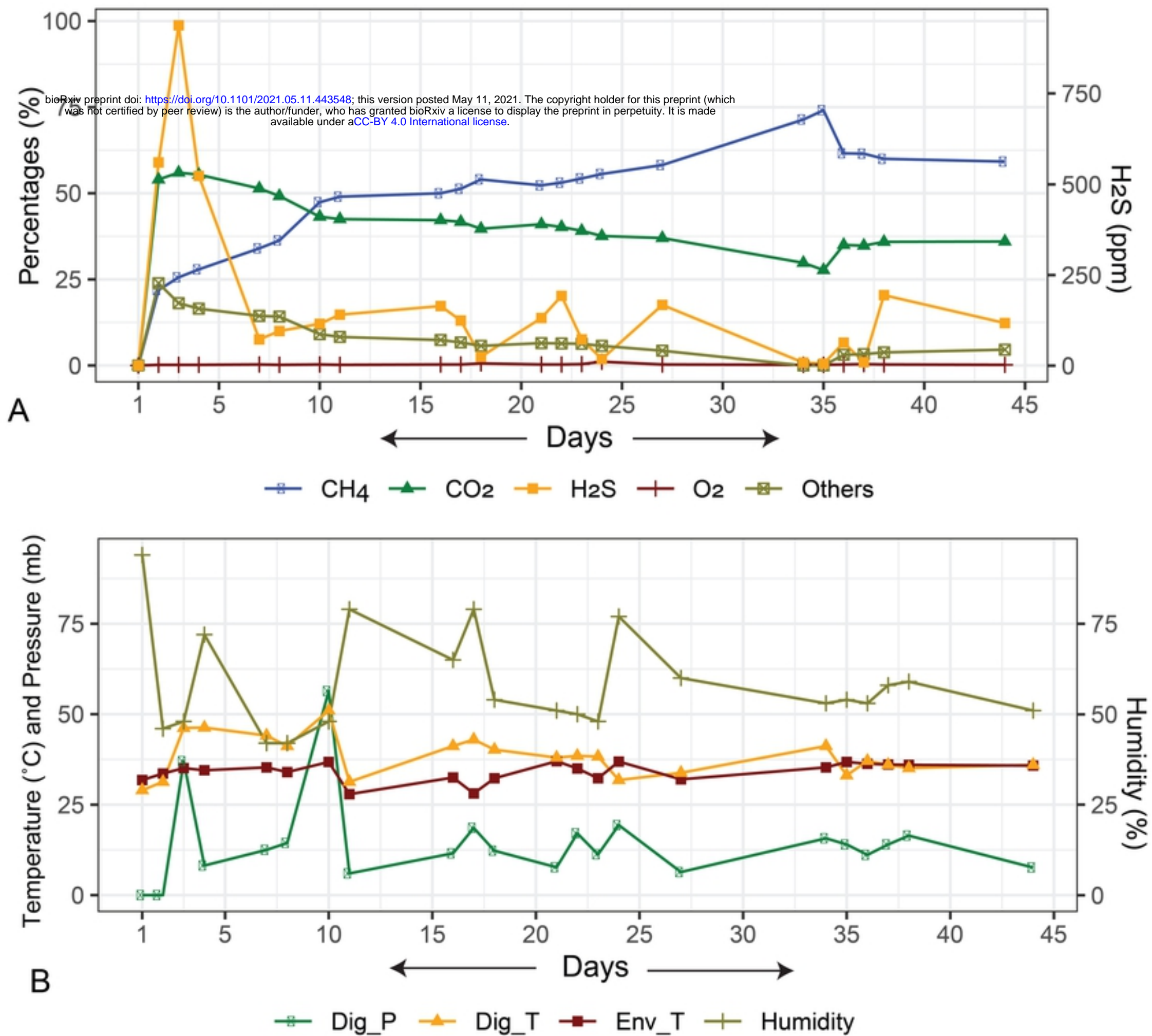
- 725 1. Khan EU, Mainali B, Martin A, Silveira S (2014) Techno-economic analysis of small scale biogas based
726 polygeneration systems: Bangladesh case study. *Sustainable Energy Technologies and*
727 *Assessments* 7: 68-78.
- 728 2. Khan EU, Martin AR (2016) Review of biogas digester technology in rural Bangladesh. *Renewable and*
729 *Sustainable Energy Reviews* 62: 247-259.
- 730 3. Weiland P (2010) Biogas production: current state and perspectives. *Applied microbiology and*
731 *biotechnology* 85: 849-860.
- 732 4. Wirth R, Kovács E, Maróti G, Bagi Z, Rákhely G, et al. (2012) Characterization of a biogas-producing
733 microbial community by short-read next generation DNA sequencing. *Biotechnology for biofuels*
734 5: 1-16.
- 735 5. Das A, Sahoo S, Rana S (2018) Sustainable conservation of kitchen wastes into fuels and organic
736 fertilizer. *International Journal of Engineering Sciences and Research Technology* 7: 503-510.
- 737 6. Agostini A, Battini F, Padella M, Giuntoli J, Baxter D, et al. (2016) Economics of GHG emissions mitigation
738 via biogas production from Sorghum, maize and dairy farm manure digestion in the Po valley.
739 *Biomass and Bioenergy* 89: 58-66.
- 740 7. Mulka R, Szulczewski W, Szlachta J, Prask H (2016) The influence of carbon content in the mixture of
741 substrates on methane production. *Clean Technologies and Environmental Policy* 18: 807-815.
- 742 8. Tian Z, Cabrol L, Ruiz-Filippi G, Pullammanappallil P (2014) Microbial ecology in anaerobic digestion at
743 agitated and non-agitated conditions. *PLOS one* 9: e109769.
- 744 9. Campanaro S, Treu L, Rodriguez-R LM, Kovalovszki A, Ziels RM, et al. (2020) New insights from the biogas
745 microbiome by comprehensive genome-resolved metagenomics of nearly 1600 species
746 originating from multiple anaerobic digesters. *Biotechnology for biofuels* 13: 1-18.
- 747 10. Valentinuzzi F, Cavani L, Porfido C, Terzano R, Pii Y, et al. (2020) The fertilising potential of manure-
748 based biogas fermentation residues: Pelleted vs. liquid digestate. *Heliyon* 6: e03325.
- 749 11. Fernandez-Gonzalez N, Braz G, Regueiro L, Lema J, Carballa M (2020) Microbial invasions in sludge
750 anaerobic digesters. *Applied Microbiology and Biotechnology*: 1-13.
- 751 12. Zhu X, Campanaro S, Treu L, Seshadri R, Ivanova N, et al. (2020) Metabolic dependencies govern
752 microbial syntrophies during methanogenesis in an anaerobic digestion ecosystem. *Microbiome*
753 8: 1-14.
- 754 13. Theuerl S, Klang J, Hülsemann B, Mächtigt T, Hassa J (2020) Microbiome Diversity and Community-Level
755 Change Points within Manure-based small Biogas Plants. *Microorganisms* 8: 1169.
- 756 14. Ziels RM, Svensson BH, Sundberg C, Larsson M, Karlsson A, et al. (2018) Microbial rRNA gene
757 expression and co-occurrence profiles associate with biokinetics and elemental composition in
758 full-scale anaerobic digesters. *Microbial biotechnology* 11: 694-709.
- 759 15. Mukti RF, Sinthee SS (2019) Metagenomic Approach: Transforming In-Silico Research for Improved
760 Biogas Production. *International Journal of Applied Sciences and Biotechnology* 7: 6-11.
- 761 16. Kemausuor F, Adaramola MS, Morken J (2018) A review of commercial biogas systems and lessons for
762 Africa. *Energies* 11: 2984.
- 763 17. Bremges A, Maus I, Belmann P, Eikmeyer F, Winkler A, et al. (2015) Deeply sequenced metagenome
764 and metatranscriptome of a biogas-producing microbial community from an agricultural
765 production-scale biogas plant. *Gigascience* 4: s13742-13015-10073-13746.
- 766 18. Ziganshin AM, Ziganshina EE, Kleinstaub S, Nikolausz M (2016) Comparative analysis of
767 methanogenic communities in different laboratory-scale anaerobic digesters. *Archaea* 2016.
- 768 19. Pham JV, Yilma MA, Feliz A, Majid MT, Maffetone N, et al. (2019) A review of the microbial production
769 of bioactive natural products and biologics. *Frontiers in microbiology* 10: 1404.

- 770 20. Sundberg C, Al-Soud WA, Larsson M, Alm E, Yekta SS, et al. (2013) 454 pyrosequencing analyses of
771 bacterial and archaeal richness in 21 full-scale biogas digesters. *FEMS microbiology ecology* 85:
772 612-626.
- 773 21. Hahnke S, Langer T, Klocke M (2018) *Proteiniborus indolifex* sp. nov., isolated from a thermophilic
774 industrial-scale biogas plant. *International journal of systematic and evolutionary microbiology*
775 68: 824-828.
- 776 22. Hoque M, Das Z, Rahman A, Haider M, Islam M (2018) Molecular characterization of *Staphylococcus*
777 *aureus* strains in bovine mastitis milk in Bangladesh. *International journal of veterinary science*
778 *and medicine* 6: 53-60.
- 779 23. Saha O, Hoque MN, Islam OK, Rahaman M, Sultana M, et al. (2020) Multidrug-resistant avian
780 pathogenic *Escherichia coli* strains and association of their virulence genes in Bangladesh.
781 *Microorganisms* 8: 1135.
- 782 24. Zhang Q, Wang M, Ma X, Gao Q, Wang T, et al. (2019) High variations of methanogenic microorganisms
783 drive full-scale anaerobic digestion process. *Environment international* 126: 543-551.
- 784 25. Hoque MN, Istiaq A, Clement RA, Gibson KM, Saha O, et al. (2020) Insights into the resistome of bovine
785 clinical mastitis microbiome, a key factor in disease complication. *Frontiers in Microbiology* 11:
786 860.
- 787 26. Hoque MN, Istiaq A, Clement RA, Sultana M, Crandall KA, et al. (2019) Metagenomic deep sequencing
788 reveals association of microbiome signature with functional biases in bovine mastitis. *Scientific*
789 *reports* 9: 1-14.
- 790 27. De Vrieze J, Christiaens ME, Walraedt D, Devooght A, Ijaz UZ, et al. (2017) Microbial community
791 redundancy in anaerobic digestion drives process recovery after salinity exposure. *Water research*
792 111: 109-117.
- 793 28. Hoque MN, Istiaq A, Rahman MS, Islam MR, Anwar A, et al. (2020) Microbiome dynamics and genomic
794 determinants of bovine mastitis. *Genomics* 112: 5188-5203.
- 795 29. Sparks DL, Page A, Helmke P, Loeppert RH (2020) *Methods of soil analysis, part 3: Chemical methods:*
796 *John Wiley & Sons.*
- 797 30. Afilal M, Elasi O, Merzak Z (2014) Caractérisations des déchets organiques et évaluation du potentiel
798 Biogaz (Organic waste characterization and evaluation of its potential biogas). *J Mater Environ Sci*
799 5: 2014.
- 800 31. Banerjee P, Prasad B (2020) Determination of concentration of total sodium and potassium in surface
801 and ground water using a flame photometer. *Applied Water Science* 10: 1-7.
- 802 32. El Asri O, Afilal ME, Laiche H, Elfarh A (2020) Evaluation of physicochemical, microbiological, and
803 energetic characteristics of four agricultural wastes for use in the production of green energy in
804 Moroccan farms. *Chemical and Biological Technologies in Agriculture* 7: 1-11.
- 805 33. Hong C, Manimaran S, Shen Y, Perez-Rogers JF, Byrd AL, et al. (2014) PathoScope 2.0: a complete
806 computational framework for strain identification in environmental or clinical sequencing
807 samples. *Microbiome* 2: 1-15.
- 808 34. Glass EM, Wilkening J, Wilke A, Antonopoulos D, Meyer F (2010) Using the metagenomics RAST server
809 (MG-RAST) for analyzing shotgun metagenomes. *Cold Spring Harbor Protocols* 2010: pdb.
810 prot5368.
- 811 35. Wood DE, Lu J, Langmead B (2019) Improved metagenomic analysis with Kraken 2. *Genome biology*
812 20: 257.
- 813 36. Li H (2018) Minimap2: pairwise alignment for nucleotide sequences. *Bioinformatics* 34: 3094-3100.
- 814 37. Li H, Durbin R (2010) Fast and accurate long-read alignment with Burrows–Wheeler transform.
815 *Bioinformatics* 26: 589-595.
- 816 38. Li H, Handsaker B, Wysoker A, Fennell T, Ruan J, et al. (2009) The sequence alignment/map format and
817 SAMtools. *Bioinformatics* 25: 2078-2079.

- 818 39. Koh H (2018) An adaptive microbiome α -diversity-based association analysis method. *Scientific reports*
819 8: 1-12.
- 820 40. Beck J, Holloway JD, Schwanghart W (2013) Undersampling and the measurement of beta diversity.
821 *Methods in Ecology and Evolution* 4: 370-382.
- 822 41. McMurdie PJ, Holmes S (2013) phyloseq: an R package for reproducible interactive analysis and
823 graphics of microbiome census data. *PloS one* 8: e61217.
- 824 42. De Cáceres M, Legendre P, Wiser SK, Brotons L (2012) Using species combinations in indicator value
825 analyses. *Methods in Ecology and Evolution* 3: 973-982.
- 826 43. Doster E, Lakin SM, Dean CJ, Wolfe C, Young JG, et al. (2020) MEGARes 2.0: a database for classification
827 of antimicrobial drug, biocide and metal resistance determinants in metagenomic sequence data.
828 *Nucleic acids research* 48: D561-D569.
- 829 44. Kanehisa M, Sato Y, Furumichi M, Morishima K, Tanabe M (2019) New approach for understanding
830 genome variations in KEGG. *Nucleic acids research* 47: D590-D595.
- 831 45. Tanimu MI, Ghazi TIM, Harun MR, Idris A (2015) Effects of feedstock carbon to nitrogen ratio and
832 organic loading on foaming potential in mesophilic food waste anaerobic digestion. *Applied*
833 *microbiology and biotechnology* 99: 4509-4520.
- 834 46. Agustini CB, da Costa M, Gutterres M (2020) Biogas from Tannery Solid Waste Anaerobic Digestion Is
835 Driven by the Association of the Bacterial Order Bacteroidales and Archaeal Family
836 Methanosaetaceae. *Applied biochemistry and biotechnology*: 1-12.
- 837 47. Liu T, Sun L, Müller B, Schnürer A (2017) Importance of inoculum source and initial community
838 structure for biogas production from agricultural substrates. *Bioresource technology* 245: 768-
839 777.
- 840 48. Zandvoort MH, van Hullebusch ED, Gieteling J, Lens PN (2006) Granular sludge in full-scale anaerobic
841 bioreactors: trace element content and deficiencies. *Enzyme and microbial technology* 39: 337-
842 346.
- 843 49. Muturi SM, Muthui LW, Njogu PM, Onguso JMa, Wachira FN, et al. (2021) Metagenomics survey
844 unravels diversity of biogas microbiomes with potential to enhance productivity in Kenya. *Plos*
845 *one* 16: e0244755.
- 846 50. Stolze Y, Zakrzewski M, Maus I, Eikmeyer F, Jaenicke S, et al. (2015) Comparative metagenomics of
847 biogas-producing microbial communities from production-scale biogas plants operating under
848 wet or dry fermentation conditions. *Biotechnology for biofuels* 8: 1-18.
- 849 51. Schmidt A, Müller N, Schink B, Schleheck D (2013) A proteomic view at the biochemistry of syntrophic
850 butyrate oxidation in *Syntrophomonas wolfei*. *PloS one* 8: e56905.
- 851 52. Lynd LR, Weimer PJ, Van Zyl WH, Pretorius IS (2002) Microbial cellulose utilization: fundamentals and
852 biotechnology. *Microbiology and molecular biology reviews* 66: 506-577.
- 853 53. Luo G, Fotidis IA, Angelidaki I (2016) Comparative analysis of taxonomic, functional, and metabolic
854 patterns of microbiomes from 14 full-scale biogas reactors by metagenomic sequencing and
855 radioisotopic analysis. *Biotechnology for biofuels* 9: 1-12.
- 856 54. Sun L, Pope PB, Eijsink VG, Schnürer A (2015) Characterization of microbial community structure during
857 continuous anaerobic digestion of straw and cow manure. *Microbial biotechnology* 8: 815-827.
- 858 55. Hanreich A, Schimpf U, Zakrzewski M, Schlüter A, Benndorf D, et al. (2013) Metagenome and
859 metaproteome analyses of microbial communities in mesophilic biogas-producing anaerobic
860 batch fermentations indicate concerted plant carbohydrate degradation. *Systematic and applied*
861 *microbiology* 36: 330-338.
- 862 56. Kouzuma A, Tsutsumi M, Ishii Si, Ueno Y, Abe T, et al. (2017) Non-autotrophic methanogens dominate
863 in anaerobic digesters. *Scientific reports* 7: 1-13.

- 864 57. Poehlein A, Schneider D, Soh M, Daniel R, Seedorf H (2018) Comparative genomic analysis of members
865 of the genera *Methanosphaera* and *Methanobrevibacter* reveals distinct clades with specific
866 potential metabolic functions. *Archaea* 2018.
- 867 58. Shcherbakova V, Rivkina E, Pecheritsyna S, Laurinavichius K, Suzina N, et al. (2011) *Methanobacterium*
868 *arcticum* sp. nov., a methanogenic archaeon from Holocene Arctic permafrost. *International*
869 *journal of systematic and evolutionary microbiology* 61: 144-147.
- 870 59. Kor-Bicakci G, Ubay-Cokgor E, Eskicioglu C (2020) Comparative analysis of bacterial and archaeal
871 community structure in microwave pretreated thermophilic and mesophilic anaerobic digesters
872 utilizing mixed sludge under organic overloading. *Water* 12: 887.
- 873 60. Cho S-K, Im W-T, Kim D-H, Kim M-H, Shin H-S, et al. (2013) Dry anaerobic digestion of food waste under
874 mesophilic conditions: performance and methanogenic community analysis. *Bioresource*
875 *Technology* 131: 210-217.
- 876 61. Deng S, Wipf HM-L, Pierroz G, Raab TK, Khanna R, et al. (2019) A plant growth-promoting microbial
877 soil amendment dynamically alters the strawberry root bacterial microbiome. *Scientific reports* 9:
878 1-15.
- 879 62. Dinova N, Belouhova M, Schneider I, Rangelov J, Topalova Y (2018) Control of biogas production
880 process by enzymatic and fluorescent image analysis. *Biotechnology & Biotechnological*
881 *Equipment* 32: 366-375.

882
883
884
885
886
887
888
889
890
891
892
893
894
895
896
897
898
899
900
901
902
903
904
905
906
907
908
909



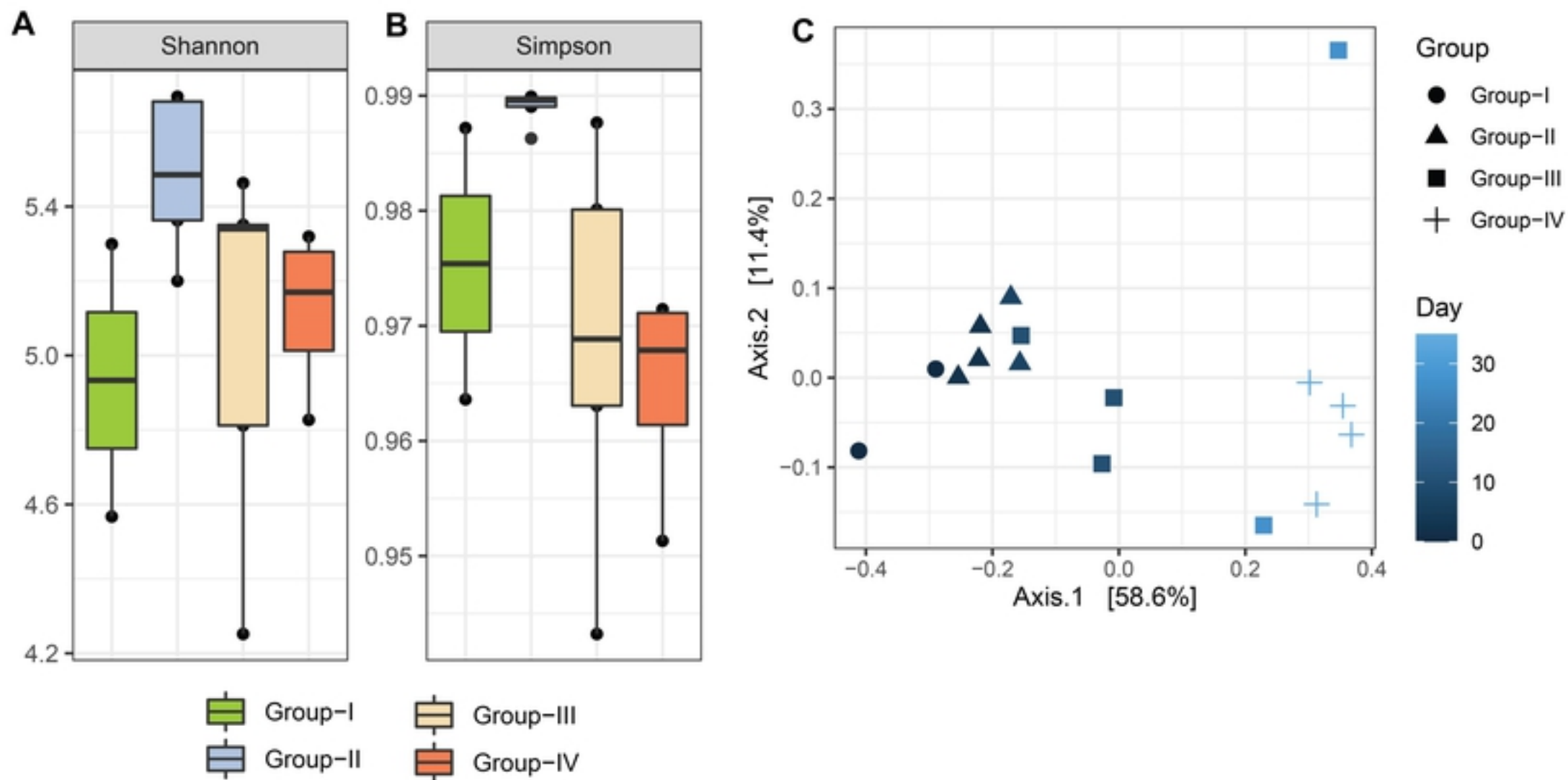


Fig. 2

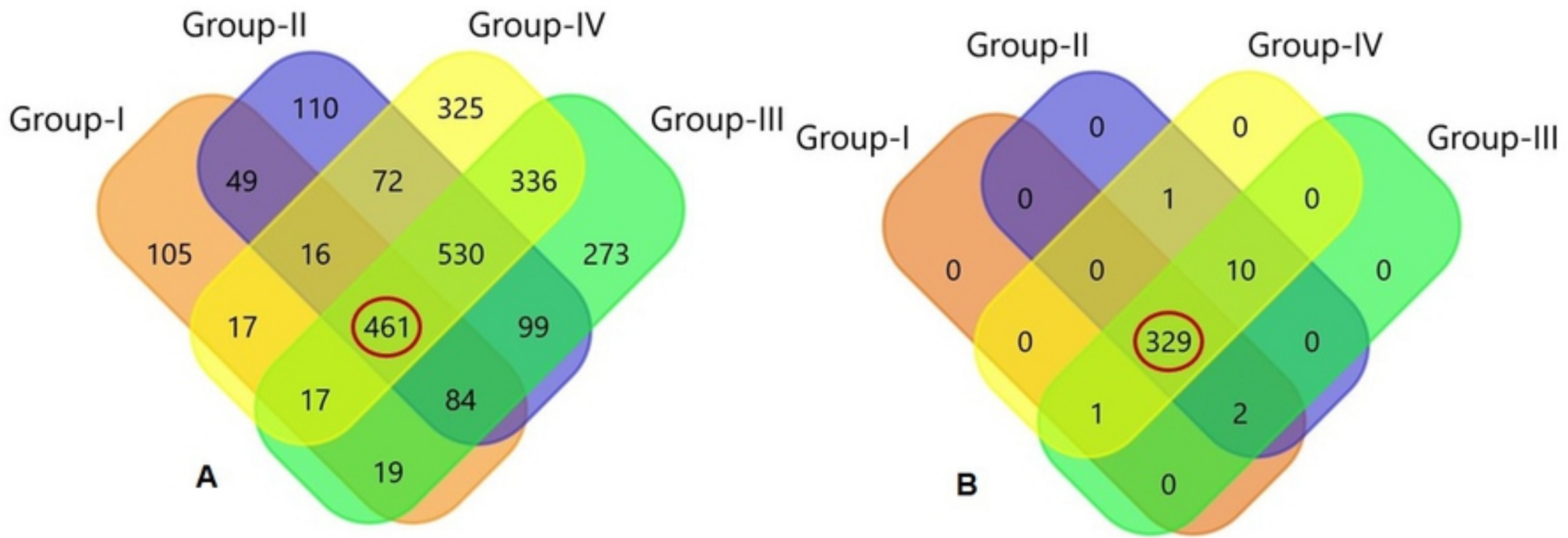


Fig. 3

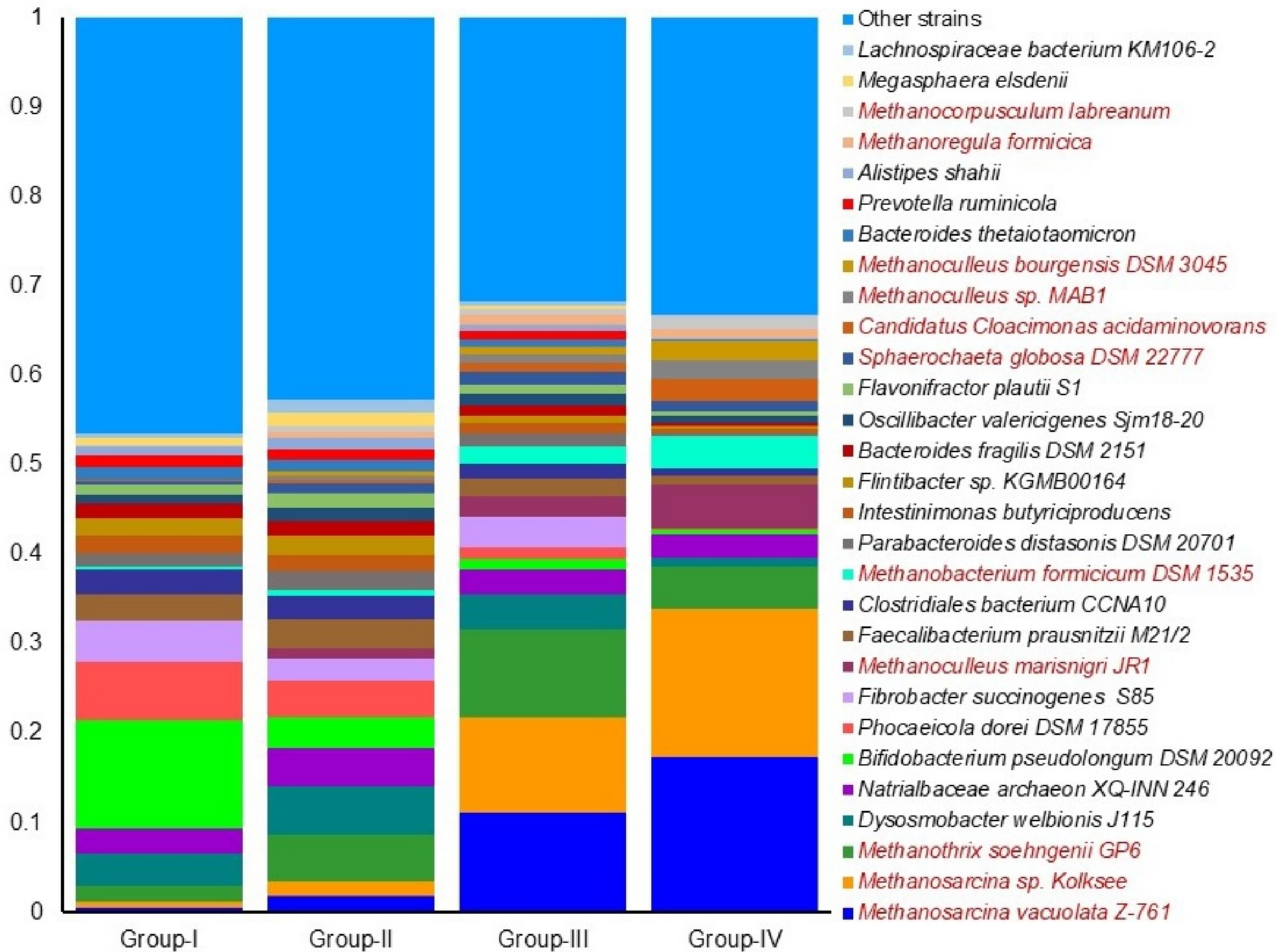


Fig. 4

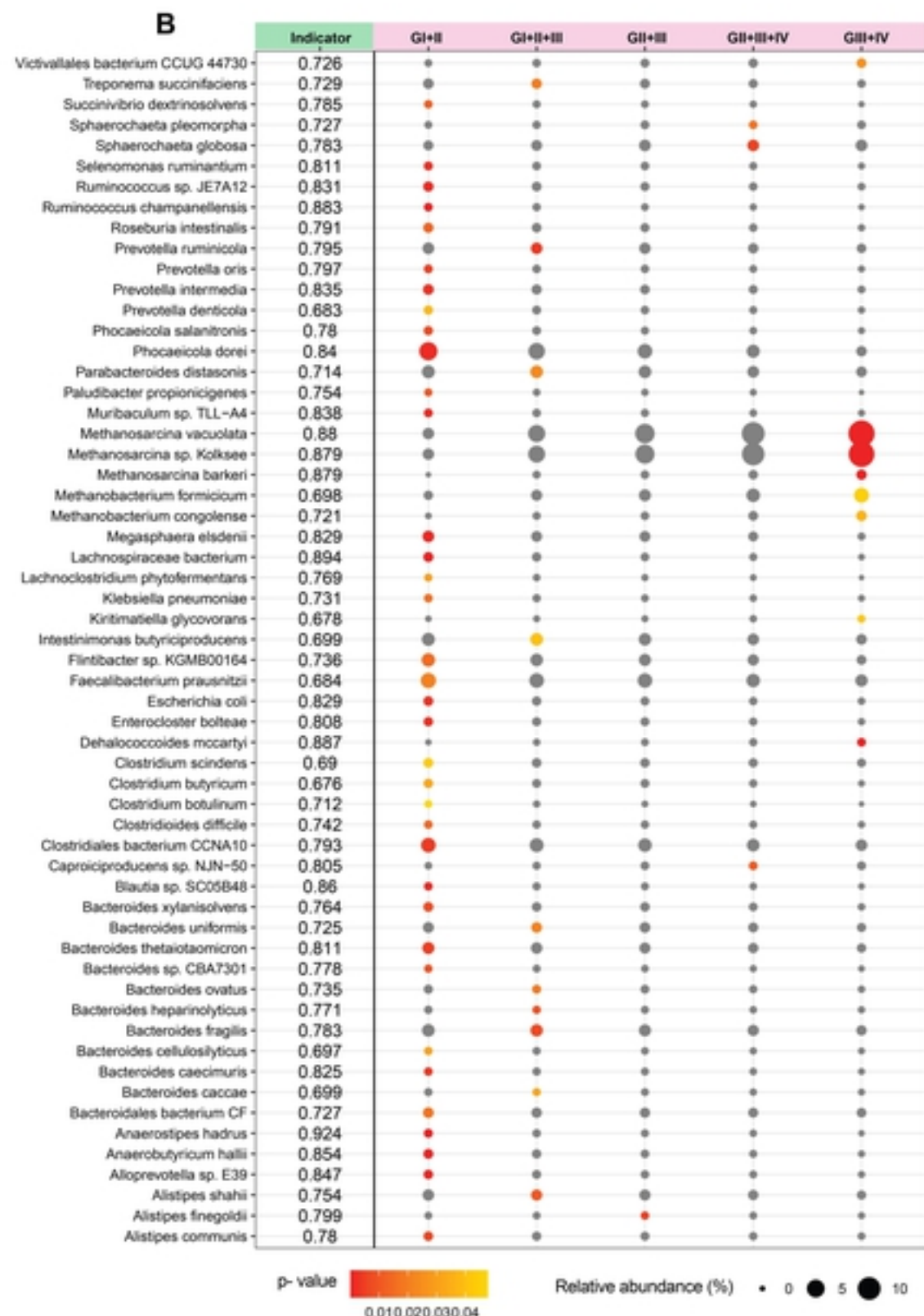
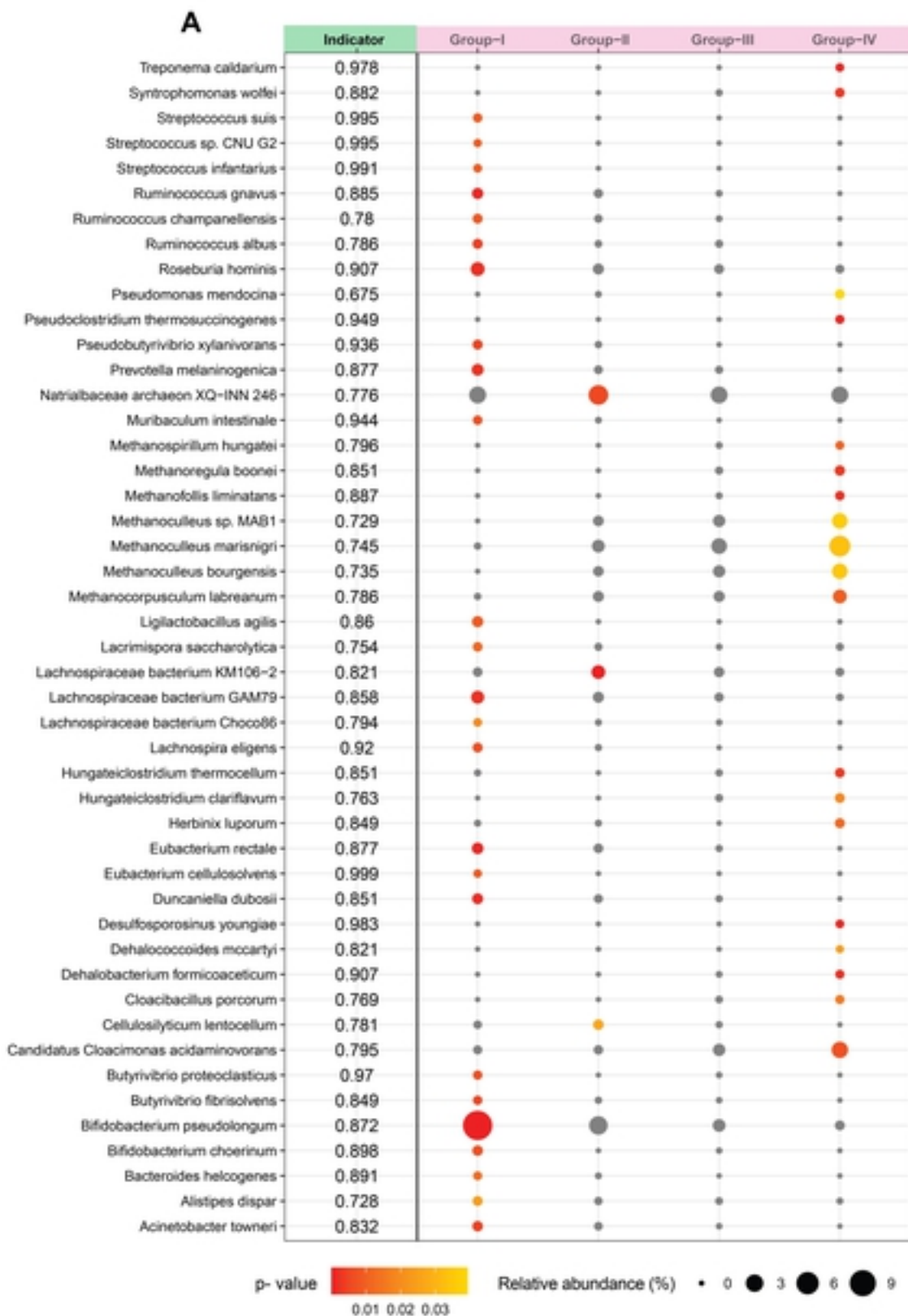


Fig. 5

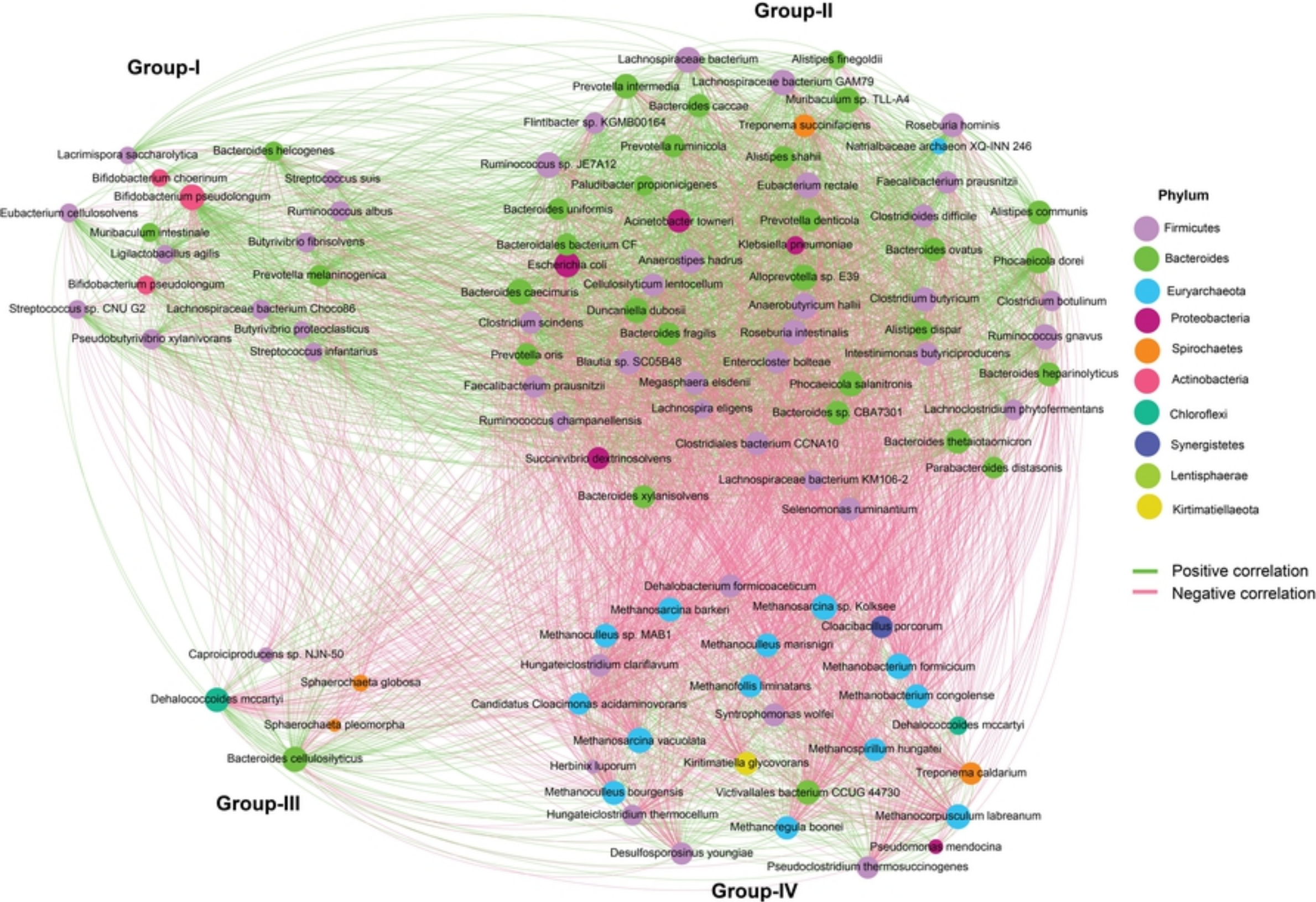


Fig. 6

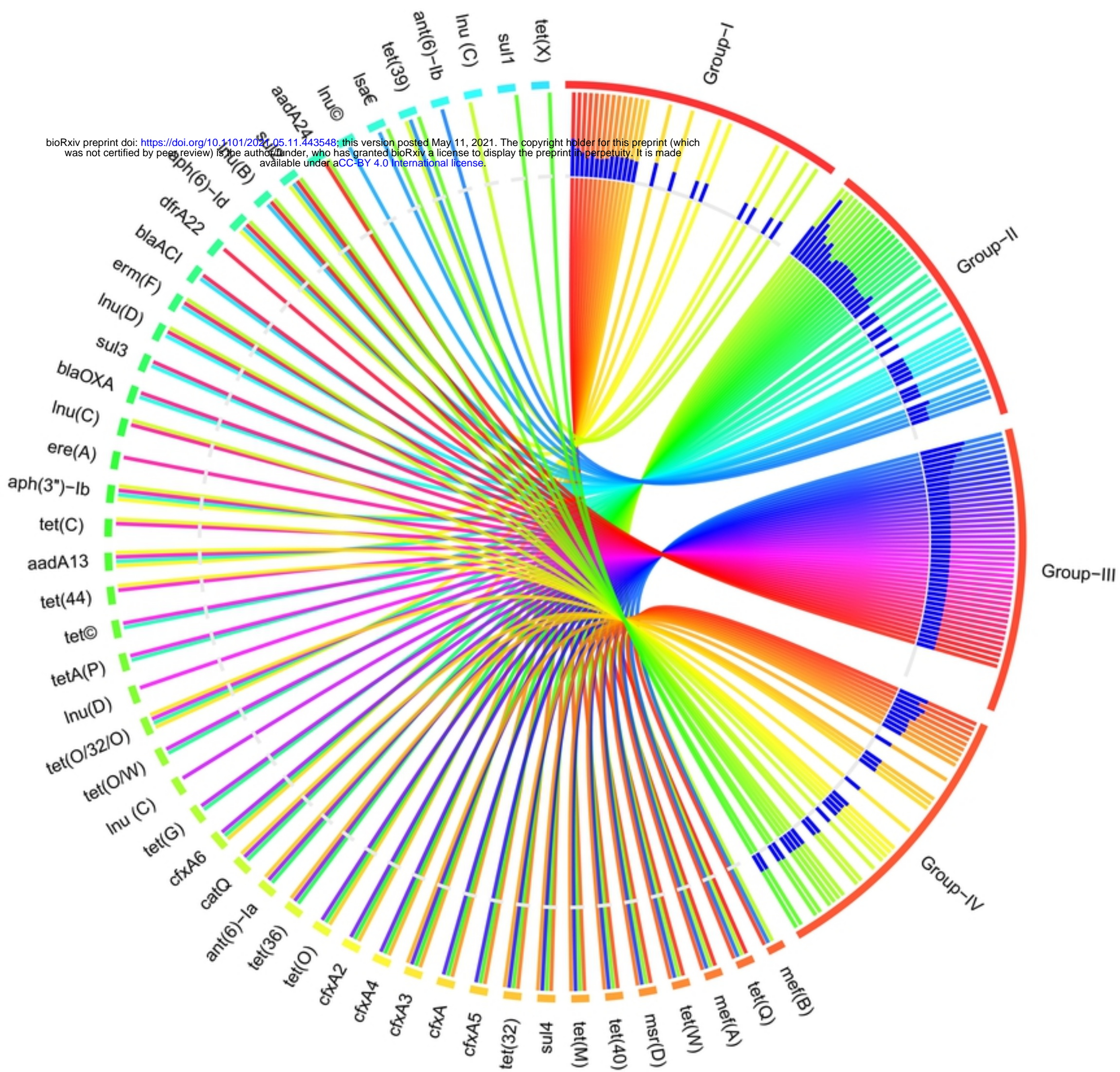


Fig. 7

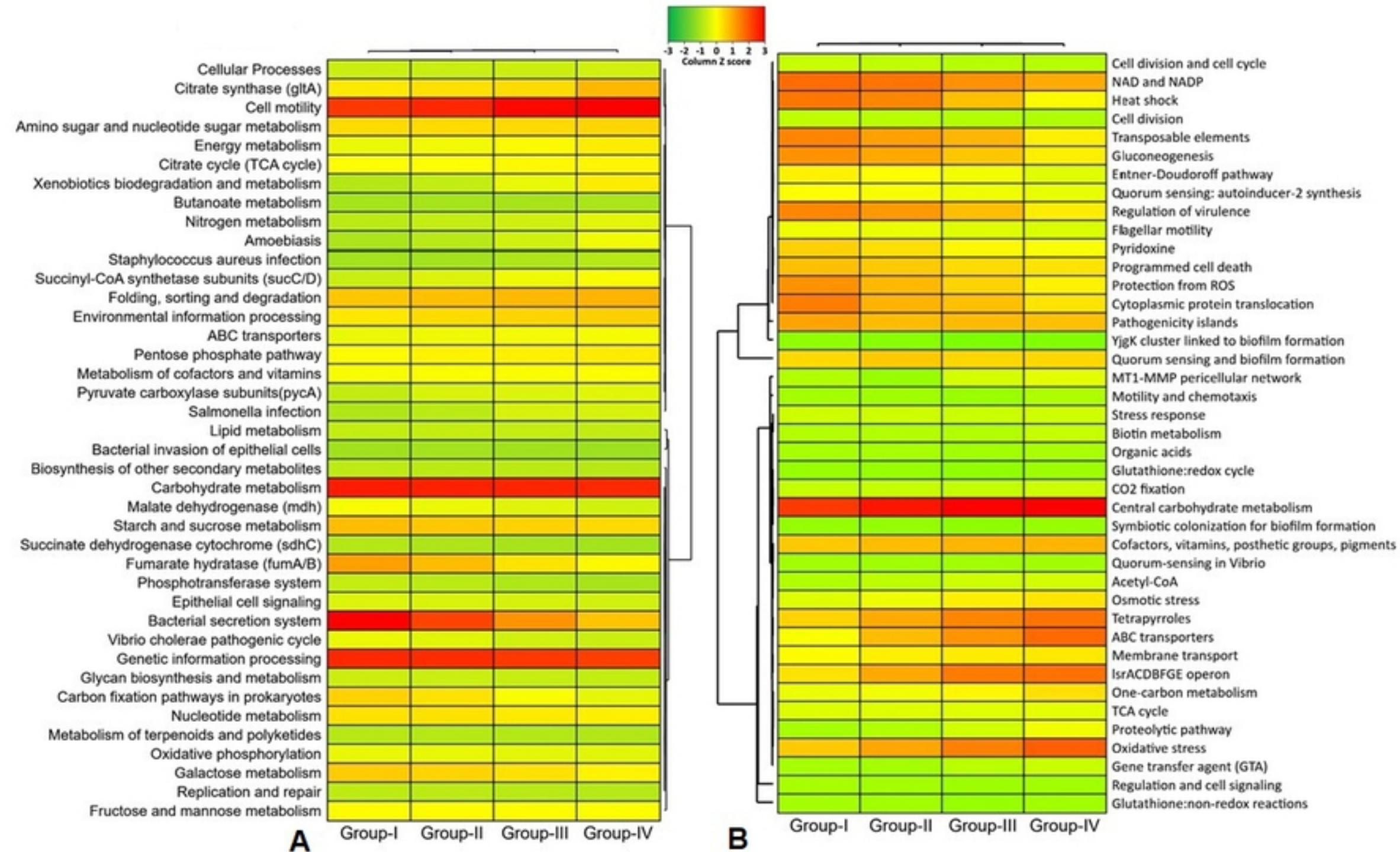


Fig. 8